A Generalized Analytical Framework for SMPT in a Multicode CDMA Wireless System (Extended Version)

Manjunath Krishnam Martin Reisslein

Abstract

Simultaneous MAC Packet Transmission (SMPT) has recently been proposed for stabilizing the throughput over wireless links, which is one of the key challenges in providing high-quality wireless multimedia services. SMPT stabilizes the wireless link by transmitting multiple packets on multiple CDMA channels in parallel in response to packet drops due to wireless link errors. These parallel packet transmissions stabilize the link layer throughput, but they also increase the interference level in a given cell of a cellular network or cluster of an ad-hoc network, which in turn reduces the number of traffic flows that can be simultaneously supported in a cell/cluster. We have recently developed an analytical framework for the class of SMPT mechanisms for a simple Bernoulli packet generation process, which does not reflect the oftentimes bursty packet generation processes encountered in real networks. In this paper we develop a *generalized* analytical framework for SMPT, which accommodates bursty packet traffic (and also non-bursty Bernoulli traffic). This framework expresses the system dynamics in transition probabilities for a Markov chain and calculates the effects of the interference through an iterative approach. The numerical results from our analytical framework and verifying simulations indicate that SMPT provides a significant reduction in packet loss and buffer occupancies (and delay), especially for persistent traffic bursts, in exchange for a reduced number of supported flows. Our analytical framework quantifies these system trade-offs with good accuracy and can thus be employed for resource management.

Keywords

ARQ, Buffer Occupancy, Bursty Packet Traffic, Capacity, Link Layer QoS, Multicode CDMA, Packet Loss Probability.

I. Introduction

Simultaneous MAC Packet Transmission (SMPT) is a novel class of Automatic Repeat reQuest (ARQ) mechanisms, which is designed to stabilize the throughput over wireless links and thus to enable high-quality wireless multimedia services [1]. SMPT exploits the parallel code channels provided by multicode CDMA, which is the basis for many modern wireless systems, e.g., IS-95 (Rev B) [2] and UMTS [3]. In contrast to conventional ARQ mechanisms, such as send-and-wait, go-back-N, and selective repeat, which transmit one packet at a time over the radio front end of the sender, SMPT transmits multiple packets in parallel. With SMPT, a sender simultaneously uses multiple CDMA code channels to transmit multiple packets in parallel

Supported in part by the National Science Foundation through grant Career ANI-0133252 and the State of Arizona through the IT301 initiative.

Please direct correspondence to M. Reisslein. M. Krishnam and M. Reisslein are with the Dept. of Electrical Eng., Arizona State University, Goldwater Center, MC5706, Tempe, AZ 85287-5706, USA, phone:(480)965-8593, fax:(480)965-8325, e-mail: {manjunath, reisslein}@asu.edu, web: http://www.fulton.asu.edu/~mre.

in response to packet drops due to errors on the wireless links. These parallel packet transmissions keep the packet backlog in the sender buffer small and thus the delay and the probability of packet loss due to buffer overflow are also kept small and thus can serve as a basis for offering high-quality multimedia services over the wireless links. SMPT operates exclusively at the link layer and does not require a central controller or scheduler. Instead, a given wireless terminal adjusts its number of used CDMA codes in response to the success or failure of its own packet transmissions. SMPT is thus well suited for the communication among uncoordinated wireless terminals in *ad hoc* networks.

The improved packet level performance of SMPT comes at the expense of increased interference levels due to the increased use of CDMA codes, which we assume throughout to be correlated pseudonoise codes. The increased interference levels tend to increase the probabilities of wireless errors and thus more frequent packet drops on the wireless links. More failed packet transmissions in turn call for the use of even more codes in SMPT, which will clearly lead to instability when the traffic level exceeds a critical threshold (the so-called capacity). With the class of SMPT ARQ mechanisms there is thus a trade-off between improved link layer packet quality of service (QoS) and a reduced number of packet flows that are provided with this higher level of QoS.

The concept of SMPT ARQ protocols opens up a new design space of policies for adjusting the number of used CDMA code channels to overcome packet drops on the wireless links. The thorough exploration of this design space and the optimization of the policies for adjusting the number of used CDMA codes for specific wireless settings requires a fundamental understanding of the dynamics of the class of SMPT mechanisms. Also, the deployment of SMPT protocols requires accurate quantitative characterizations of the link layer QoS and the number of supported flows for resource allocation in wireless systems running a form of SMPT. Towards providing a basis for the exploration and optimization of SMPT policies and the resource allocation for SMPT, we have developed in [1] an analytical framework for SMPT. A key limitation of the analytical framework developed in [1] is that it accommodates only non-bursty uncorrelated packet generation, more specifically, it is limited to a Bernoulli packet generation process. In practical wireless systems, however, the link layer packet traffic is oftentimes bursty and correlated due to bursty application traffic [4], [5] and the fragmentation of higher layer protocol data units (e.g., IP datagrams) into smaller link layer protocol data units (which we refer to as packets).

In this paper we develop a *generalized* analytical framework for the class of SMPT protocols, which accommodates non-bursty (Bernoulli) packet traffic as well as bursty packet traffic. In particular, we consider Markov modulated Bernoulli processes, which are a common model for bursty packet traffic at the wireless link layer [6], [7]. In contrast to our analysis for Bernoulli traffic, which evaluated the client buffer occupancy and number of used channels directly from the dynamics of SMPT, our generalized analytical framework expresses the dynamics of SMPT in transition probabilities which are used to formulate a

Markov chain model of the SMPT system. Whereas the simpler Bernoulli traffic allowed us to calculate the interference level directly, we adopt an iterative approach to calculate the interference level and its impact on the client buffer occupancies for the more complicated bursty traffic considered in this paper. We find in our numerical evaluations that the iterative approach converges very quickly (typically after three to four iterations). Similar to the analytical framework developed in [1], the analytical framework developed in this paper is modular in nature and thus provides insights into the key drivers of the SMPT system dynamics and allowing for the characterization of new forms of SMPT.

This paper is structured as follows. In the following subsection we review related work. In Section II we give an overview of the considered multicode CDMA system and the class of SMPT ARQ mechanisms. We describe the considered network architecture, client traffic model as well as wireless link model. We also define our performance metrics which are the client buffer occupancy and the buffer overflow (packet loss) probability. In Section III we present our generalized analytical framework. We first give an overview of the analytical framework and then evaluate the transition probabilities for the various SMPT system dynamics, including the client buffer occupancy and number of used CDMA codes. We then describe the calculation of the interference level used in our iterative approach. In Section IV we present illustrative numerical results obtained from our analytical framework and verifying simulations for slow healing SMPT, an elementary form of SMPT. We summarize our conclusions in Section V.

A. Related Work

Most closely related to our study are the lines of work on the link (medium access control) layer analysis of ARQ mechanisms in wireless systems and on providing link layer QoS in wireless multicode CDMA systems.

The classical ARQ mechanisms for a *single wireless channel* have been analyzed thoroughly, see for instance [6], [7], [8], [9], [10]. The studied ARQ mechanisms include hybrid ARQ schemes that combine some form of forward error correction with ARQ, see e.g., [11], [12], as well as ARQ schemes that adapt to channel variations, see for instance [13], [14], [15], [16], [17], [18], [19], [20], [21], [22], [23]. These hybrid ARQ studies are largely orthogonal to our study on SMPT. We envision that SMPT's packet transmissions over the multiple parallel CDMA code channels may be combined with FEC to form hybrid SMPT schemes. We also envision that channel adaptive mechanisms (in addition to SMPT's underlying channel adaptive packet transmission/re-transmission) may be added to those hybrid SMPT schemes. We leave these directions to be explored in future work.

Closer related to our work are the studies on providing link layer QoS in multicode CDMA systems. A conceptual framework for a multicode CDMA based wireless multimedia network which mentions the possibility of conducting ARQ retransmissions over a separate CDMA code channel, but does not analyze

this approach is presented in [24]. Admission control strategies for multiple traffic classes (each requiring a different, but fixed number of code channels) in a multicode CDMA system are studied in [25]. A hybrid ARQ scheme for transmitting video in a multicode CDMA system is developed and analyzed in [26]. In this scheme, the number of code channels used by a given client is constant. If packets are lost, the scheme reduces the level of forward error correction, and thus increases the transmission (bit) rate for payload data to accommodate retransmissions on the fixed number of CDMA code channels. A scheme for video transmission in multicode CDMA systems is also studied in [27], which is similar to SMPT in that multiple codes are used in parallel on a dynamic basis. The main difference between [27] and SMPT is that [27] requires a significant amount of coordination among the videos being transmitted (for instance, the video streams are aligned such that a (typically large) Intracoded (I)-frame of one video stream does not coincide with the I-frame of another video stream). SMPT on the other hand does not require any coordination among the ongoing traffic flows, and is thus well suited for wireless networks with little or no coordination among the wireless terminals, such as ad-hoc networks.

We finally note that a number of schemes have been developed for providing link layer QoS in wireless multicode CDMA systems with a fixed infra-structure and a *central* base-station, see for instance [28], [29] (which are based on the DQRUMA [30]) or the LIDA/BALI approach [31], [32] as well as the more recent studies [33], [34], [35], [36], [37]. In contrast, SMPT mechanisms are distributed, i.e., SMPT does not require a central unit for packet scheduling, and is thus well suited for ad-hoc wireless networks.

II. Overview of Multicode CDMA System and SMPT

In this section we give an overview of the considered wireless multicode CDMA wireless system and the class of SMPT protocols. The wireless system and the protocols considered in this paper are essentially the same as in [1], with the main difference that we consider a more realistic and more general packet traffic model in this paper. We review therefore the properties of the considered wireless system and the class of SMPT protocols only briefly and refer to [1] for more details.

SMPT packet transmission mechanisms do not require any coordination between the transmitting terminals and thus can be deployed in cellular networks as well as ad-hoc networks. To fix ideas for our analysis we consider the uplink communication in a cellular system as illustrated in Figure 1. In the considered system, J wireless (and possibly mobile) terminals transmit to the base-station using multicode CDMA whereby each wireless terminal uses a set of unique pseudo noise code sequences. We suppose that the clients belong to K classes whereby the clients in a given class $k,\ k = 1, \ldots, K$, have similar characteristics. More specifically, we let J_k denote the number of clients (terminals) in class k, whereby $\sum_{k=1}^{K} J_k = J$. We let $R_{\max,k},\ k = 1, \ldots, K$, denote the number of parallel code channels supported by clients in class k and assume throughout perfect power control, ensuring that each wireless terminal is received at the base-

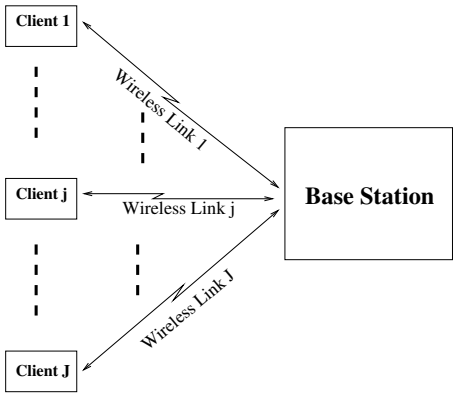

Fig. 1. System Architecture: J wireless clients conduct uncoordinated uplink transmissions to a base-station.

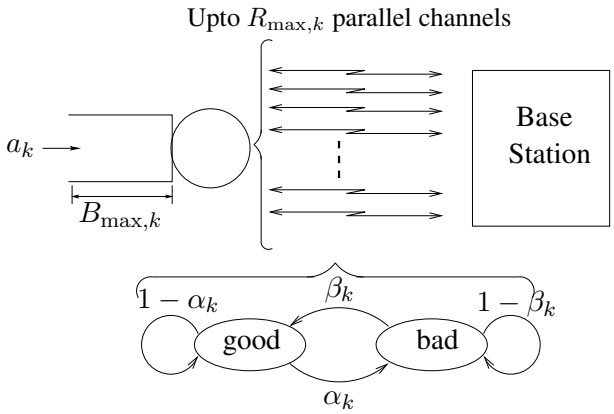

Fig. 2. The client j belonging to class k has a buffer of capacity $B_{\max,k}$ packets and is served by upto $R_{\max,k}$ parallel code channels. The wireless link (consisting of upto $R_{\max,k}$ channels) is modeled with a two-state Markov chain.

station with the same power level (which is typical for modern wireless systems [38]). We consider a system with a time division duplex (TDD) timing structure, where time is divided into fixed-length *slots*. Each slot is sub-divided into a fixed-length *uplink subslot* followed by a *downlink subslot* of fixed-length. The uplink subslot is used for transmissions in the uplink direction, i.e., from the wireless terminals to the base station, whereas the downlink subslot is used for transmissions in the opposite direction.

We assume that the wireless terminals transmit fixed-size packets (link layer protocol data units) to the base-station. The packet size is set such that one CDMA code channel accommodates exactly one packet in one uplink subslot. By using its $R_{\max,k}$ parallel code channels, a terminal belonging to class k can send up to $R_{\max,k}$ packets in an uplink subslot.

A. Client Architecture and Traffic Generation

Each of the clients of class k has a buffer of capacity $B_{\max,k}$ packets as illustrated in Figure 2. We consider both a simple non-bursty Bernoulli packet generation process as well as a bursty Markov modulated Bernoulli packet generation process. With the non-bursty process, a client of class k generates a new packet independently with probability $a_k,\ 0 < a_k \leq 1$, at the beginning of an uplink subslot.

Bursty traffic at the link layer arises in practice due to the combination of (i) bursty application traffic [4], [5], and (ii) the fragmentation of higher layer protocol data units (IP datagrams) into smaller link layer protocol data units (referred to as packets in this paper). Following [6], [7] we model the bursty traffic at the link layer of a client j belonging to class $k,\ k = 1, \ldots, K$, by an independent two-state Markov chain with the states "active" and "inactive", as illustrated in Figure 3. These Markov chains make state transitions at the end of every downlink subslot. The state transition probabilities are denoted by λ_k and μ_k as illustrated

in Figure 3. We let $X_j(n)$ be a random variable denoting the activity state (either active or inactive) of client

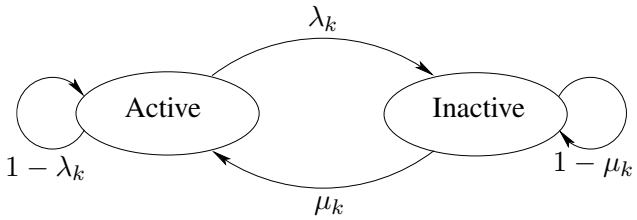

Fig. 3. The bursty traffic at the link layer of each client is modeled with an independent two-state Markov chain.

j belonging to class k in slot n. We let X_j denote the corresponding steady state random variable. A client in the active state generates a new packet at the beginning of an uplink subslot with probability one, whereas in the inactive state no new packets are generated. Note that the long run average probability of packet generation in a slot is $\mu_k/(\lambda_k + \mu_k)$. Also, note that the average burst length of $1/\lambda_k$ packets increases as λ_k decreases. In other words, for smaller λ_k the traffic becomes more bursty.

A newly generated packet is placed in the client buffer; if the buffer is full the packet is lost. Packets are transmitted in the uplink subslot out of the client's buffer to the base-station according to the SMPT mechanisms discussed in Section II-D. Each of the packets successfully transmitted in the up-link subslot is acknowledged by the base station in the subsequent down-link subslot, which is feasible with typical hardware configurations [39]. All the acknowledged packets are immediately flushed from the buffer and the unacknowledged packets remain in the buffer. The client will attempt to re-transmit the unacknowledged packet(s) in the following uplink subslot(s) according to some form of SMPT.

B. Note on Notation

Before we proceed further, a note on the notation used throughout this paper is in order. We consider K classes of clients, whereby the clients of a given class have identical system parameters (which include the maximum number of used codes, the transition probabilities for the activity state, etc.) but behave stochastically independently. We therefore index the random variables describing the client behavior with the client index j, as for instance in $X_j(n)$ and X_j. We note however, that the steady state random variables of the client behavior for the clients in a given class are independent and identically distributed (IID) random variables, e.g., the $X_j,\ j = 1, \ldots, J_k$ are IID for a given class $k,\ k = 1, \ldots, K$. For brevity we could refer to each such collection of IID random variables for a given class k with one random variable indexed with the class index k. However, for clarity, we prefer (i) to explicitly refer to the individual random variables for the client behavior with the client index j, and (ii) to explicitly state the affiliation of client j to a given class k throughout the paper.

C. Wireless Link Model

We employ the widely used two-state Markov chain model [40], [41], which captures the correlated errors that are typical for wireless links as our basic underlying wireless link model. We model the wireless link (consisting of up to $R_{\max,k}$ parallel code channels) between each wireless terminal belonging to class k and the base-station as an independent discrete time Markov Chain with two states: "good" and "bad". In the good state, packet transmissions are generally successful. However, to capture the interference between the ongoing transmissions, we drop a packet in the good state with a probability that is a function of the interference level as discussed in more detail shortly. The bad state corresponds to a deep fade (or shadowing) in which all packet transmissions are unsuccessful. This two-state model has been found to be a useful and accurate model for link layer (packet level) analysis [10], [42], [43], [44], [45], [46] and may be obtained from more complex wireless channel models, which may incorporate adaptive error control techniques, using weak lumpability or stochastic bounding techniques [47]. While we model the J wireless links in the cell as J independent Markov Chains, we do introduce dependencies between the links when modeling the link errors in the good state. These dependencies capture the interference between the ongoing transmissions in the cell, as detailed shortly.

In our channel model, state transitions occur at the end of each downlink subslot. We refer to a slot during which the wireless link of client j belonging to class k is in the good (bad) state as a *good (bad) slot* for the link. Throughout we assume that all parallel code channels of a given wireless link (between a particular client and the base-station) experience either a good slot or a bad slot. We denote α_k for the probability that a transition takes the link of client j in class k from the good state to the bad state, given that the link is currently in the good state (with the complementary probability $1-\alpha_k$ the link stays in the good state), as illustrated in Fig. 2. We denote β_k for the link's transition probability from the bad state to the good state. We let $C_j(n)$ be a random variable denoting the state (either good or bad) of link j in slot n and denote C_j for the corresponding steady state random variable.

We denote the interference level experienced by a client j in class k during the uplink transmission in slot n, i.e., the total number of codes used by the other clients in this subslot, by $\mathcal{I}_j(n),\ 0 \leq \mathcal{I}_j(n) \leq (J_k-1)\cdot R_{\max,k} + \sum_{l=1,l\neq k}^{K} J_l \cdot R_{\max,l}$. We assume here that the codes of a given client are orthogonal, achieved for instance by sub-code concatenation, such that there is no self-interference and only the remaining J_k-1 clients in class k interfere with client j, plus all J_l clients from all the other classes $l,\ l=1,\ldots,K, l\neq k$. We calculate the interference level $\mathcal{I}_j(n)$, as a function of the channel states of the clients interfering with the transmissions of client j in class k, as detailed in Section III. For convenience we introduce the following notation for this analysis for client j in class k. We let $G_k(n),\ 0 \leq G_k(n) \leq J_k-1$, denote the number of other clients (i.e., not counting client j) in class k which experience a good channel in slot n. We let $G_l(n),\ l=1,\ldots,K, l\neq k$, with $0 \leq G_l(n) \leq J_l$, denote the number of clients in class l which experience

a good channel in slot n. We define the vector $\mathbf{G}_j(n)$ to denote the number of other clients (not counting client j in class k) that experiencing a good channel in slot n

$$\mathbf{G}_j(n) = \{G_1(n),\ G_2(n),\ \ldots,\ G_k(n),\ \ldots,\ G_K(n)\}. \tag{1}$$

This vector will be used in our analytical framework for the calculation of the interference level of client j in Section III-B, where we distinguish between the interferers (other clients) that experience a good channel and those that experience a bad channel.

In our link model we evaluate the probability $q_{good,j}(\mathcal{I}_j(n))$ that a packet sent from client j to the base station in a good slot n is dropped as a function of the interference level $\mathcal{I}_j(n)$. We employ the widely used Holtzman approximation [48] to calculate the bit error probability $q_{bit,j}(\mathcal{I}_j(n))$ resulting from the interference level $\mathcal{I}_j(n)$. Based on the bit error probability $q_{bit,j}(\cdot)$ we calculate the packet drop probability in the good state $q_{good,j}(\mathcal{I}_j(n))$ by considering an elementary FEC scheme as detailed in [1].

We note that the interference level $\mathcal{I}_j(n)$ in turn is a function of the numbers of interfering clients with good/bad channel conditions, expressed by the vector $\mathbf{G}_j(n)$, and the statistics of the number of code channels used by clients with good/bad channel conditions in the individual classes, as detailed in Section III-B. For notational convenience we denote this functional dependence of the packet drop probability by $q_{pkt,j}[\mathbf{G}_j(n)]$ and employ this notation in the formulation of the Markov chain model in Section III. We detail in Section III-B how to obtain $q_{pkt,j}[\mathbf{G}_j(n)]$ from $q_{good,j}(\cdot)$.

Note that the outlined link modeling captures the interference effect of the ongoing uplink transmissions in a cell in the models for the individual wireless links, i.e., a given client "feels" the transmissions of the other clients in the cell. We emphasize that we use the Holtzman approximation for the bit error probability and the elementary FEC for the packet error probability only to fix ideas. Our analytical framework only assumes that there is some way to obtain the packet drop probability $q_{good,j}(\cdot)$ as a function of the number of interfering codes $\mathcal{I}_j(n)$.

D. Overview of SMPT

Packet transmission with SMPT differs from packet transmission with conventional ARQ mechanisms (send-and-wait, go-back-N, and selective repeat) in that SMPT transmits multiple packets in parallel on multiple CDMA codes "to catch up" after suffering unsuccessful (i.e., unacknowledged) packet transmissions. Consider a client generating a sequence of packets, one per slot, and transmitting these to the base station. Suppose that one of the packets is dropped due to errors on the wireless link and not acknowledged. In response to the dropped packet, the client transmits in the next uplink subslot the dropped packet and the subsequent packet (which would have been transmitted in that subslot had there not been a packet drop) on two CDMA codes. If these two packets are successfully received and acknowledged, the client

returns to sending one packet using one CDMA code in the next uplink subslot. On the other hand, if the two packets are not successfully acknowledged, the client sends the two packets plus the newly generated packet using three parallel CDMA codes. This "ramping up" process continues until the backlogged packets are successfully transmitted or the maximum number of parallel codes $R_{\max,k}$ is reached. This outlined SMPT mechanisms is referred to as *basic SMPT*, which performs well for uncorrelated occurrences of bad slots. For correlated bad slots, however, basic SMPT is inefficient as it increases the number of used codes (interference level) during a run of consecutive bad slots without reducing the backlog. To overcome this shortcoming, forms of SMPT with *link probing* have been introduced. The client enters the link probing mode when all packets sent in a given uplink slot are dropped. While probing the link, the client sends only one of the dropped packets as a link probe using a single CDMA code channel until this packet is successful. (Physical layer techniques could be used instead of the link probe to assess the status of the link. However, we are interested in the fundamental link layer performance characteristics of SMPT with respect to conventional ARQ mechanisms and consider therefore link probing.) When the probing packet is successfully acknowledged the client leaves the link probing mode and ramps up the number of used CDMA codes to clear the backlog. Different forms of ramping up the number of used CDMA codes are possible. With the so-called *slow healing* SMPT, the client ramps up by adding one CDMA code for each slot up to the maximum of $R_{\max,k}$ codes. We note that many other forms of SMPT can be designed by varying the way in which the number of parallel CDMA code channels are adjusted. We consider slow healing SMPT as an illustrative example of a from of SMPT with link probing in this paper and consider this form of SMPT in our numerical investigations in Section IV. However, we emphasize that the analysis techniques developed for SMPT mechanisms in the Section III are general and can be applied to any form of SMPT. In the analysis, we let $R_j(n),\ 0 \leq R_j(n) \leq R_{\max,k}$, be a random variable denoting the number of parallel code channels used by client j belonging to class k for the uplink transmission in slot n. We denote R_j for the corresponding steady state random variable.

E. Performance Metrics

In this section we define the performance metrics considered in our analysis of SMPT. We focus primarily on the occupancy of the client buffer and the buffer overflow (packet loss) probability. We let $B_j(n),\ 0 \leq B_j(n) \leq B_{\max,k}$, be a random variable denoting the buffer occupancy (in number of packets) in client j belonging to class k at the beginning of slot n (before the packet newly generated at the beginning of slot n joins the buffer). We let B_j denote the corresponding steady state random variable. We define the packet loss probability $P_{\text{loss}}(j)$ for client j in class k as the probability that a given newly generated packet finds the buffer full, i.e., $P_{\text{loss}}(j) = P(B_j = B_{\max,k})$. We define the average loss probability among the clients

in the cell as

$$P_{\text{loss}} = \frac{1}{J}\sum_{j=1}^{J} P_{\text{loss}}(j). \tag{2}$$

III. Generalized Analytical Framework

In this section we present our generalized analytical framework for SMPT. The framework accommodates any form of SMPT that adjusts the number of CDMA code channel used in a slot as a function of the buffer occupancy in the current slot and the number of used code channels in the immediately preceding slot, i.e., any form that has a one-step memory. (The analysis can be extended to longer memories at the expense of increased complexity). At the core of the analytical framework is a Markov chain. In describing this Markov chain we focus on a given client j belonging to class k. A state of the Markov chain for client j is characterized by (i) the activity state $X_j(n)$, (ii) the link state $C_j(n)$, (iii) the number of used code channels $R_j(n)$, (iv) the buffer occupancy $B_j(n)$, and (v) the channel states of the interferers $\mathbf{G}_j(n)$ of client j, i.e., the states of the Markov chain for client j in class k are given by the 5-tuples $\{X_j(n), C_j(n), R_j(n), B_j(n), \mathbf{G}_j(n)\}$. Note that the state space of the Markov chain has $2 \cdot 2 \cdot (R_{\max,k}+1) \cdot (B_{\max,k}+1) \cdot J_k \cdot \Pi_{l=1,l\neq k}^{K}(J_l+1)$ states, which for typical wireless systems can be readily accommodated by contemporary PC technology. We evaluate the transition probabilities $Pr\{X_j(n+1), C_j(n+1), R_j(n+1), B_j(n+1), \mathbf{G}_j(n+1) \mid X_j(n), C_j(n), R_j(n), B_j(n), \mathbf{G}_j(n)\}$ of the irreducible and aperiodic Markov chain for client j as detailed in Section III-A. We then obtain the steady state joint probability distribution $Pr\{X_j, C_j, R_j, B_j, \mathbf{G}_j\}$ using standard techniques. From this joint distribution we obtain the various distributions of interest, e.g., the probability distribution of the client buffer occupancy $Pr\{B_j\}$, which gives the loss probability $P_{\text{loss}}(j)$, with standard techniques.

The key challenge in the analysis is to account for the interference, which we capture with the following iterative approach. We initially assume that the interference experienced by each client is negligible (i.e., $q_{pkt,j}[\cdot] = 0$) and perform the outlined Markov chain analysis for each class k to obtain the distributions of the channel usage conditioned on the channel states for the clients in each class $Pr\{R_j|C_j\}$. From these conditional channel usage distributions we calculate the interference levels and packet drop probabilities $q_{pkt,j}[\cdot]$ as detailed in Section III-B. With these packet drop probabilities we perform another iteration of the Markov chain analysis and re-evaluate the channel usage distributions and interference levels. We continue iterating until the interference levels do not change significantly, which typically requires only three to four iterations.

A. Evaluation of Transition Probabilities

In this section we evaluate the transition probabilities required for the Markov chain analysis outlined above. We first note that the channel state $C_j(n+1)$ and the transition probabilities of the client activity

state $X_j(n+1)$ are each mutually independent of the other system states. We also note that the buffer occupancy $B_j(n+1)$ depends only on $B_j(n),\ X_j(n),\ C_j(n),\ R_j(n)$, and $q_{pkt,j}[\mathbf{G}_j(n)]$. Furthermore, the number of used codes $R_j(n+1)$ depends on $R_j(n),\ C_j(n),\ B_j(n+1)$, and $X_j(n+1)$. We now proceed to evaluate the probabilities for these state transitions in detail.

A.1 Client Activity X_j and Channel State C_j

In Table I we provide the transition probabilities for the activity states of client j belonging to class k for bursty packet generation and non-bursty Bernoulli packet generation, respectively. In Table II we provide the transition probabilities for the channel state of the client. These transition probabilities follow

TABLE I

TRANSITION PROBABILITIES FOR ACTIVITY STATE OF CLIENT j BELONGING TO CLASS k

(a) Bursty packet arrivals

$X_j(n)$	$X_j(n+1)$	$Pr\{X_j(n+1)\|X_j(n)\}$
Active	Active	$1-\lambda_k$
Active	Inactive	λ_k
Inactive	Active	μ_k
Inactive	Inactive	$1-\mu_k$

(b) Non-bursty Bernoulli packet arrivals

$X_j(n)$	$X_j(n+1)$	$Pr\{X_j(n+1)\|X_j(n)\}$
Active	Active	a_k
Active	Inactive	$1-a_k$
Inactive	Active	a_k
Inactive	Inactive	$1-a_k$

TABLE II

TRANSITION PROBABILITIES FOR CHANNEL STATE OF CLIENT j BELONGING TO CLASS k

$C_j(n)$	$C_j(n+1)$	$Pr\{C_j(n+1)\|C_j(n)\}$
Good	Good	$1-\alpha_k$
Good	Bad	α_k
Bad	Good	β_k
Bad	Bad	$1-\beta_k$

all directly from the traffic and channel models presented in Sections II-A and II-C. We also note that the transition probabilities for the channel states of the clients interfering with client j are evaluated analogously as $Pr\{\mathbf{G}_j(n+1)|\mathbf{G}_j(n)\} = \Pi_{l=1}^{K} Pr\{G_l(n+1)|G_l(n)\}$. We provide a pseudocode for calculating the individual probabilities $Pr\{G_l(n+1)|G_l(n)\}$ in Figure 4. In this pseudocode we let $\mathtt{Jc}$ denote the total number of interfering clients from the considered class, i.e., $\mathtt{Jc}= J_k-1$ for class k, which client j belongs to, and $\mathtt{Jc}= J_l$ for the other classes $l,\ l=1,\ldots,K,\ l\neq k$. The pseudocode evaluates $Pr\{G_l(N+1)|G_l(n)\}$ by considering all feasible combinations of numbers of channel state transitions from good to bad denoted by $\mathtt{gb}$ and numbers of state transitions from bad to good denoted by $\mathtt{bg}$.

```
1.  for G_l(n) := 0 to Jc in steps of 1
2.    for G_l(n+1) := 0 to Jc in steps of 1
3.      Pr{G_l(n+1)|G_l(n)} := 0
4.      for index := 0 to G_l(n) in steps of 1
5.        gb := index;
6.        bg := G_l(n+1) - (G_l(n) - index);
7.        if(bg>=0) and (bg <= Jc - G_l(n))
8.          Pr{G_l(n+1)|G_l(n)} := Pr{G_l(n+1)|G_l(n)}+
9.            C(G_l(n), gb) α_l^gb (1-α_l)^(G_l(n)-gb) . C(Jc-G_l(n), bg) β_l^bg (1-β_l)^(Jc-G_l(n)-bg)
```

Fig. 4. Pseudocode for calculating $Pr\{G_l(n+1)|G_l(n)\}$

A.2 Buffer Occupancy B_j

The buffer occupancy $B_j(n+1)$ at the beginning of slot $n+1$ depends on the buffer occupancy $B_j(n)$ at the beginning of the preceding slot as well as the client activity status $X_j(n)$, the channel status $C_j(n)$, the number of used code channels $R_j(n)$, and the channel conditions experienced by the interfering clients $\mathbf{G}_j(n)$ in the preceding slot n as detailed in Table III. The channel conditions of the interfering clients $\mathbf{G}_j(n)$ along with the statistics of the channel usage of interfering clients with good/bad channels govern the probability with which a packet transmitted by client j is unsuccessful, $q_{pkt,j}[\mathbf{G}_j(n)]$, which is calculated as detailed in III-B. The transition probabilities in the table are derived from the following reasoning. If client

TABLE III
TRANSITION PROBABILITIES FOR BUFFER OCCUPANCY GIVEN $\mathbf{G}_j(n)$

$X_j(n)$	$C_j(n)$	$B_j(n+1)$	Probability
Active	Good	$\max\{\min\{B_j(n)+1, B_{\max,k}\}, 0\}$	$p\{R_j(n), 0, q_{pkt,j}[\mathbf{G}_j(n)]\}$
		$\max\{\min\{B_j(n)+1, B_{\max,k}\}-1, 0\}$	$p\{R_j(n), 1, q_{pkt,j}[\mathbf{G}_j(n)]\}$
		$\vdots$	$\vdots$
		$\max\{\min\{B_j(n)+1, B_{\max,k}\}-(R_j(n)-1), 0\}$	$p\{R_j(n), R_j(n)-1, q_{pkt,j}[\mathbf{G}_j(n)]\}$
		$\max\{\min\{B_j(n)+1, B_{\max,k}\}-R_j(n), 0\}$	$p\{R_j(n), R_j(n), q_{pkt,j}[\mathbf{G}_j(n)]\}$
Inactive	Good	$\max\{B_j(n), 0\}$	$p\{R_j(n), 0, q_{pkt,j}[\mathbf{G}_j(n)]\}$
		$\max\{B_j(n)-1, 0\}$	$p\{R_j(n), 1, q_{pkt,j}[\mathbf{G}_j(n)]\}$
		$\vdots$	$\vdots$
		$\max\{B_j(n)-(R_j(n)-1), 0\}$	$p\{R_j(n), R_j(n)-1, q_{pkt,j}[\mathbf{G}_j(n)]\}$
		$\max\{B_j(n)-R_j(n), 0\}$	$p\{R_j(n), R_j(n), q_{pkt,j}[\mathbf{G}_j(n)]\}$
Active	Bad	$\min\{B_j(n)+1, B_{\max,k}\}$	1
Inactive	Bad	$B_j(n)$	1

j is active in slot n, then the buffer occupancy is incremented by a packet; however the buffer occupancy can not exceed $B_{\max,k}$. If the client experiences a bad channel in slot n, then irrespective of the number of codes available to the client, the buffer content is not reduced in slot n. When the client experiences a good

channel in slot n, then the situation is as follows. The client transmits $R_j(n)$ packets in the slot. Each of these packets is successful with probability $1.0 - q_{pkt,j}[\mathbf{G}_j(n)]$. Thus the total number of successful packets is binomially distributed as

$$p\{R_j(n), r, q_{pkt,j}[\mathbf{G}_j(n)]\} = \binom{R_j(n)}{r} \cdot (1 - q_{pkt,j}[\mathbf{G}_j(n)])^r \cdot (q_{pkt,j}[\mathbf{G}_j(n)])^{(R_j(n)-r)} \text{ for all } r = 0, \ldots, R_j(n). \quad (3)$$

A.3 Number of Used Codes R_j

The number of codes $R_j(n+1)$ used by client j belonging to class k in slot $n+1$ depends on the number of codes used $R_j(n)$ and the channel state $C_j(n)$ in the preceding slot n as well as the buffer occupancy $B_j(n+1)$ at the beginning of slot $n+1$ and the client activity state $X_j(n+1)$ in slot $n+1$, as detailed in Tables IV and V for slow healing SMPT and basic SMPT, respectively. It is important to note that the table of the transition probabilities of R_j is the only component of our analytical framework that depends on the specific SMPT scheme used. We describe here in detail the reasoning employed to derive the transition probabilities for slow healing SMPT. The transition probabilities for basic SMPT in Table V as well as the transition probabilities for novel forms of SMPT are derived in analogous fashion. For slow healing SMPT, we first note that whenever the channel state $C_j(n)$ is bad in a slot, the number of codes used in the next slot $R_j(n+1)$ is reduced to *one* to conduct the link probing, provided there is a packet to be transmitted in the next time slot; if there is no packet to be transmitted (i.e., $B_j(n+1) = 0$), then $R_j(n+1)$ is set to *zero*. If $C_j(n)$ is good, then $R_j(n+1)$ is set depending on the activity state and buffer occupancy. More specifically, $R_j(n+1)$ is set to the minimum of $R_j(n)+1$ and $B_j(n+1)$ if $X_j(n+1)$ is inactive. On the other hand, $R_j(n+1)$ is set to the minimum of $R_j(n)+1$ and $B_j(n+1)+1$ if $X_j(n+1)$ is active. In both cases, the client can not send more packets than then number of permitted code channels ($R_j(n)+1$ with slow healing SMPT) or the number of packets in the buffer at the beginning of the slot after the packet generation for the slot ($B_j(n+1)$ if no new packet is generated at the beginning of slot $n+1$; $B_j(n+1)+1$ if a new packet is generated at the beginning of slot $n+1$). In any case, the number of used code channels can not exceed $R_{\max,k}$. Note that the described transitions of the number of used codes to $R_j(n+1)$ are deterministic functions, i.e., occur with probability one; all other $R_j(n+1)$ values are assigned a transition probability of zero .

Using the transition probability tables provided in this section, it is straightforward to evaluate the transitions probabilities $Pr\{X_j(n+1), C_j(n+1), R_j(n+1), B_j(n+1), \mathbf{G}_j(n+1) \mid X_j(n), C_j(n), R_j(n), B_j(n), \mathbf{G}_j(n)\}$, which are then employed in the Markov chain analysis as outlined at the beginning of Section III.

B. Calculating the Interference Level

In this section we explain how to calculate the probability that a packet sent by client j of class k in a good slot n is dropped on the wireless link, which we have denoted by $q_{pkt,j}[\mathbf{G}_j(n)]$. In calculating this

TABLE IV
TRANSITION OF NUMBER OF USED CODES $R_j(n+1)$ FOR SLOW HEALING SMPT.

$X_j(n+1)$	$C_j(n)$	$R_j(n+1)$
Active	Good	$\min\{R_j(n)+1,\ \min\{B_j(n+1)+1,\ B_{\max,k}\},\ R_{\max,k}\}$
Inactive	Good	$\min\{R_j(n)+1,\ B_j(n+1),\ R_{\max,k}\}$
Active	Bad	1
Inactive	Bad	$\min\{B_j(n+1), 1\}$

TABLE V
TRANSITION OF NUMBER OF USED CODES $R_j(n+1)$ FOR BASIC SMPT.

$X_j(n+1)$	$C_j(n)$	$R_j(n+1)$
Active	Good	$\min\{\min\{B_j(n+1)+1,\ B_{\max,k}\},\ R_{\max,k}\}$
Inactive	Good	$\min\{B_j(n+1),\ R_{\max,k}\}$
Active	Bad	$\min\{\min\{B_j(n+1)+1,\ B_{\max,k}\},\ R_{\max,k}\}$
Inactive	Bad	$\min\{B_j(n+1),\ R_{\max,k}\}$

probability we need to consider the interference level, i.e., the total number of codes used by the other clients in slot n. The first point to note in this calculation is that in SMPT with some form of link probing, the number of CDMA codes used by a client that is experiencing a bad channel significantly differs from the number of CDMA codes used by a client experiencing a good channel. To account for these dynamics of SMPT, we consider the channel usage distribution of clients experiencing a good channel separately from the channel usage distribution of clients experiencing a bad channel. More specifically, from our Markov chain analysis we obtain the conditional channel usage distributions $Pr\{R_i|C_i = good\}$ and $Pr\{R_i|C_i = bad\}$ for the clients i from each of the classes $l,\ l = 1, \ldots, K$. From these distributions we calculate the mean and variance of the number of CDMA codes used by a client i from a given class l conditioned on the client experiencing a good channel or a bad channel. We denote these means and variances by $\bar{R}_i^g$, σ_i^g, $\bar{R}_i^b$, and σ_i^b, respectively. We approximate the interference level caused by a client i from class l by

$$I_i^g = \bar{R}_i^g + \kappa\sigma_i^g \tag{4}$$

when the client experiences a good channel and by

$$I_i^b = \bar{R}_i^b + \kappa\sigma_i^b \tag{5}$$

when the client experiences a bad channel, where κ denotes a multiplication factor, similar to the multiplication factor used in the interference calculation in [1]. Our numerical work (see Section IV) indicates that this approximation has good accuracy for $\kappa = 1.5$.

With these interference levels we calculate $q_{pkt,j}[\mathbf{G}_j(n)]$ as follows. Let $\mathbf{G}_j(n) = \{G_1(n) = g_1,\ G_2(n) =$

$g_2, \ldots, G_k(n) = g_k, \ldots, G_K(n) = g_K\}$ with $g_k \in \{0, 1, \ldots, J_k - 1\}$ and $g_l \in \{0, 1, \ldots, J_l\}, \forall l \neq k$, denote a given combination of numbers of clients experiencing a good channel. The probability of packet failure when client j belonging to class k transmits a packet while experiencing a good channel is then approximately

$$q_{pkt,j}[\mathbf{G}_j(n)] = q_{\text{good},j} \left(g_k \cdot I_k^g + (J_k - 1 - g_k) \cdot I_k^b + \sum_{l=1, l \neq k}^{K} (g_l \cdot I_l^g + (J_l - g_l) \cdot I_l^b) \right), \tag{6}$$

which is employed in the calculation of the transition probabilities of the buffer occupancy, as detailed in Section III-A.2.

We note that when considering the above analysis it would appear that a simpler alternative would be to evaluate the expected value of the total interference level $E[\mathcal{I}_j]$ experienced by client j in class k in a good slot as

$$\begin{aligned} E[\mathcal{I}_j] &= (J_k - 1) \cdot [Pr\{C_j = good\} \cdot I_j^g + Pr\{C_j = bad\} \cdot I_j^b] + \\ &\quad \sum_{l=1, l \neq k}^{K} J_l \cdot [Pr\{C_i = good\} \cdot I_i^g + Pr\{C_i = bad\} \cdot I_i^b]. \end{aligned} \tag{7}$$

However, we found that this approach, which approximates the interference levels for the various combinations of numbers of clients with a good channel by one expected value and would eliminate the need for $\mathbf{G}_j(n)$ in the state space of the Markov chain, does not accurately capture the effects of the interference on the SMPT system. By keeping track of the combinations of numbers of clients with a good channel $\mathbf{G}_j(n)$ and calculating the interference level as described above, our analytical framework captures the dynamics of the SMPT system with good accuracy as demonstrated by the numerical examples in the next section.

In our iterative evaluation of the SMPT system we initially set $q_{pkt,j}[\cdot] = 0$ and solve for each class of clients the Markov chain to obtain the conditional channel usage distributions $Pr\{R_i|C_i\}$ and the corresponding interferences I_i^g and I_i^b. These interferences I_i^g and I_i^b are then employed in $q_{pkt,j}[\cdot]$ as given in (6) in the second iteration of the Markov chain analysis. The interferences I_i^g and I_i^b from this second iteration of the Markov chain analysis are then compared with the interferences from the previous iteration. If the differences are negligible, then the analysis terminates. On the other hand, if the differences are significant, a new iteration of the Markov chain analysis is performed with the new interferences, and so on. We found in our numerical work that three to four iterations are typically sufficient.

IV. Numerical Examples

In this section, we give a representative overview of our numerical studies of the performance of SMPT for bursty packet traffic. In the numerical examples presented here, we consider a scenario with homogeneous

clients ($K = 1$) with a buffer capacity of $B_{\max} = 20$ packets. We consider different channel parameters, the first set of parameters being $\alpha = 1/27$ and $\beta = 1/3$, and the second set being $\alpha = 1/100$ and $\beta = 1/10$. We also investigate the impact of spreading factor on the system performance, with clients having a spreading gain of 16 and 32. In contrast to [1], we consider bursty traffic with different average burst lengths $1/\lambda$, whereby we keep the utilization fixed at $\mu/(\lambda + \mu) = 0.4$. We plot the average packet loss probability P_{loss}, average system throughput $Th = \sum_{j=1}^{J} a_j \cdot [1 - P_l(j)]$, average buffer occupancy $B_{\text{avg}} = (1/J) \sum_{j=1}^{J} \sum_{b=0}^{B_{\max}} b \cdot Pr\{B_j = b\}$, and standard deviation B_{std} as a function of the number of clients J supported in the cell/cluster. We plot results obtained from our analytical framework (A) and verifying simulation results (S) which were obtained from discrete event simulations with a statistical confidence such that the 90% confidence interval is less than 10% of the corresponding sample mean. Figures 5 through 36 observe the same for a system comprising clients whose channel parameters are $\alpha = 1/27$ and $\beta = 1/3$, and a spreading gain of 16. Figures 37 through1 68 observe the same for a system comprising clients whose channel parameters are $\alpha = 1/100$ and $\beta = 1/10$. In all of these plots the varying parameters are the maximum number of codes used by the client R_j, the intensity of the burst $1/\lambda$, and the long run average activity factor of the client $\mu/(\lambda + \mu)$.

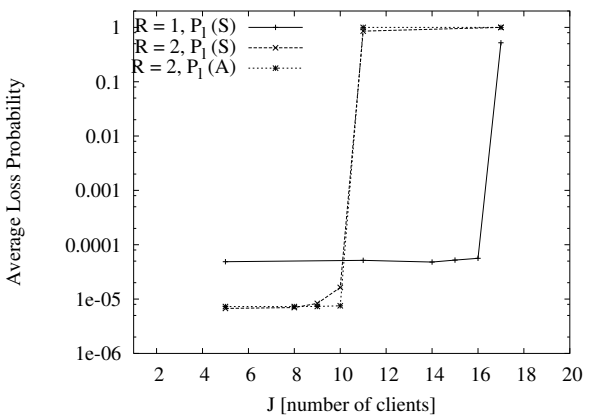

Fig. 5. Average loss probability as a function of number of supported clients (flows) J for conventional ARQ ($R = 1$) and SMPT with $R = 2$ (bursty traffic with $\mu/(\lambda + \mu) = 0.4$, $1/\lambda = 10$, $B_{\max} = 20$ packets, Spreading Gain $G = 16$, and channel conditions $\alpha = 1/27$ and $\beta = 1/3$, fixed).

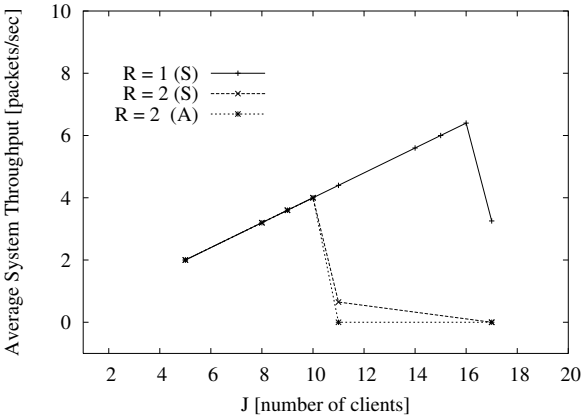

Fig. 6. Aggregate throughput as a function of number of supported clients (flows) J for conventional ARQ ($R = 1$) and SMPT with $R = 2$ (bursty traffic with $\mu/(\lambda + \mu) = 0.4$ and $1/\lambda = 10$, $B_{\max} = 20$ packets, Spreading Gain $G = 16$, and channel conditions $\alpha = 1/27$ and $\beta = 1/3$, fixed).

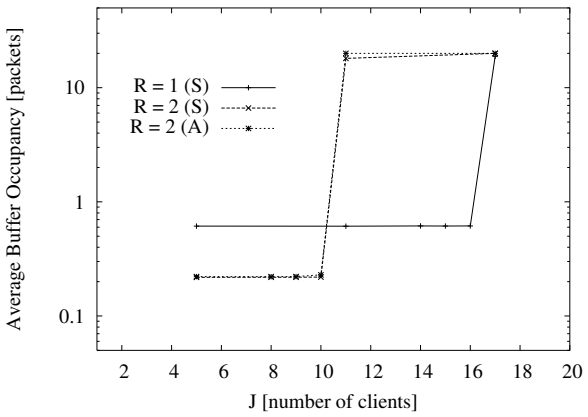

Fig. 7. Average buffer occupancy as a function of number of supported clients (flows) J for conventional ARQ ($R = 1$) and SMPT with $R = 2$ (bursty traffic with $\mu/(\lambda + \mu) = 0.4$, $1/\lambda = 10$, $B_{\max} = 20$ packets, Spreading Gain $G = 16$, and channel conditions $\alpha = 1/27$ and $\beta = 1/3$, fixed).

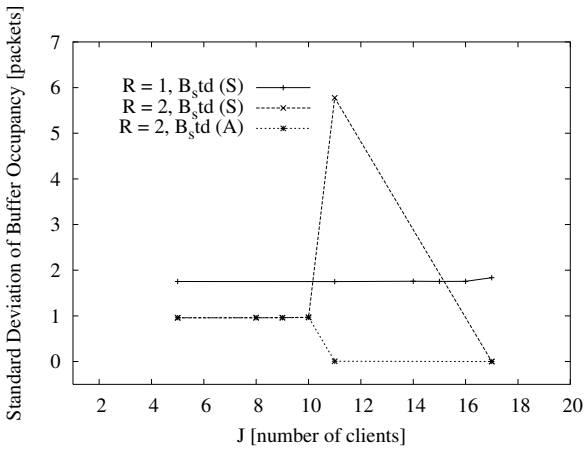

Fig. 8. Standard Deviation of buffer occupancy as a function of number of supported clients (flows) J for conventional ARQ ($R = 1$) and SMPT with $R = 2$ (bursty traffic with $\mu/(\lambda + \mu) = 0.4$ and $1/\lambda = 10$, $B_{\max} = 20$ packets, Spreading Gain $G = 16$, and channel conditions $\alpha = 1/27$ and $\beta = 1/3$, fixed).

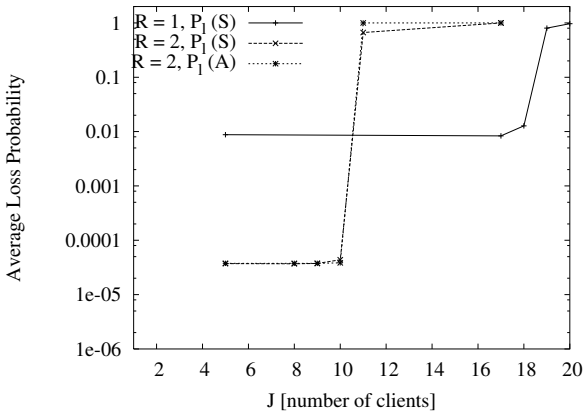

Fig. 9. Average loss probability as a function of number of supported clients (flows) J for conventional ARQ ($R = 1$) and SMPT with $R = 2$ (bursty traffic with $\mu/(\lambda + \mu) = 0.4$, $1/\lambda = 100$, $B_{\max} = 20$ packets, Spreading Gain $G = 16$, and channel conditions $\alpha = 1/27$ and $\beta = 1/3$, fixed).

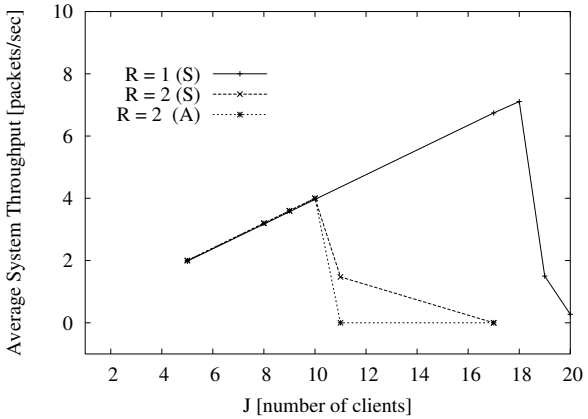

Fig. 10. Aggregate throughput as a function of number of supported clients (flows) J for conventional ARQ ($R = 1$) and SMPT with $R = 2$ (bursty traffic with $\mu/(\lambda+\mu) = 0.4$ and $1/\lambda = 100$, $B_{\max} = 20$ packets, Spreading Gain $G = 16$, and channel conditions $\alpha = 1/27$ and $\beta = 1/3$, fixed).

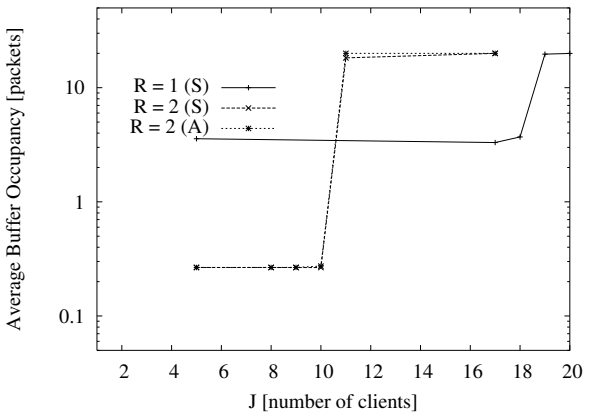

Fig. 11. Average buffer occupancy as a function of number of supported clients (flows) J for conventional ARQ ($R = 1$) and SMPT with $R = 2$ (bursty traffic with $\mu/(\lambda+\mu) = 0.4$, $1/\lambda = 100$, $B_{\max} = 20$ packets, Spreading Gain $G = 16$, and channel conditions $\alpha = 1/27$ and $\beta = 1/3$, fixed).

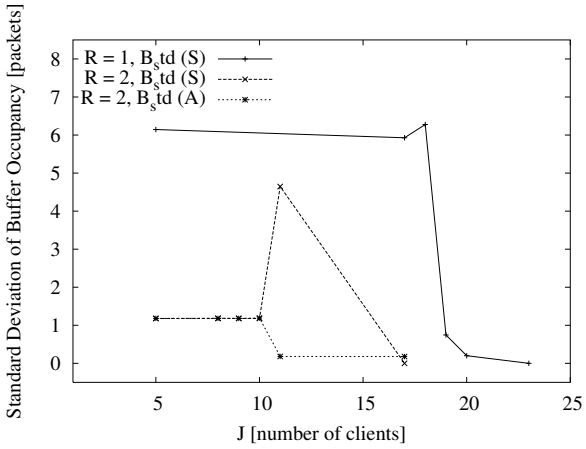

Fig. 12. Standard Deviation of buffer occupancy as a function of number of supported clients (flows) J for conventional ARQ ($R = 1$) and SMPT with $R = 2$ (bursty traffic with $\mu/(\lambda+\mu) = 0.4$ and $1/\lambda = 100$, $B_{\max} = 20$ packets, Spreading Gain $G = 16$, and channel conditions $\alpha = 1/27$ and $\beta = 1/3$, fixed).

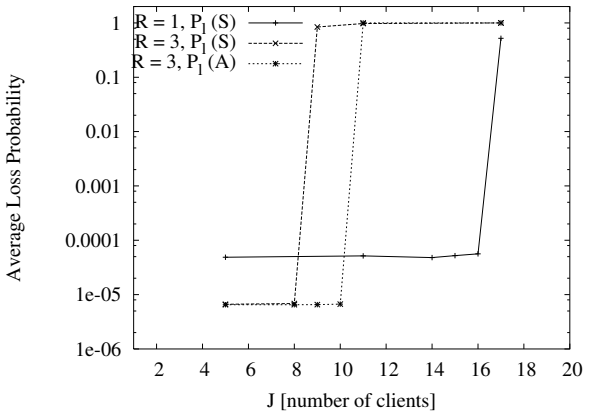

Fig. 13. Average loss probability as a function of number of supported clients (flows) J for conventional ARQ ($R = 1$) and SMPT with $R = 3$ (bursty traffic with $\mu/(\lambda+\mu) = 0.4$, $1/\lambda = 10$, $B_{\max} = 20$ packets, Spreading Gain $G = 16$, and channel conditions $\alpha = 1/27$ and $\beta = 1/3$, fixed).

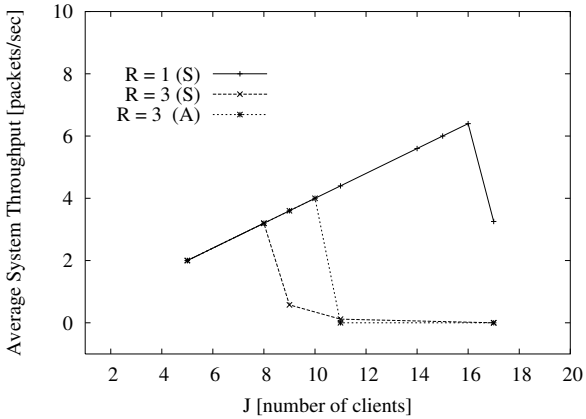

Fig. 14. Aggregate throughput as a function of number of supported clients (flows) J for conventional ARQ ($R = 1$) and SMPT with $R = 3$ (bursty traffic with $\mu/(\lambda+\mu) = 0.4$ and $1/\lambda = 10$, $B_{\max} = 20$ packets, Spreading Gain $G = 16$, and channel conditions $\alpha = 1/27$ and $\beta = 1/3$, fixed).

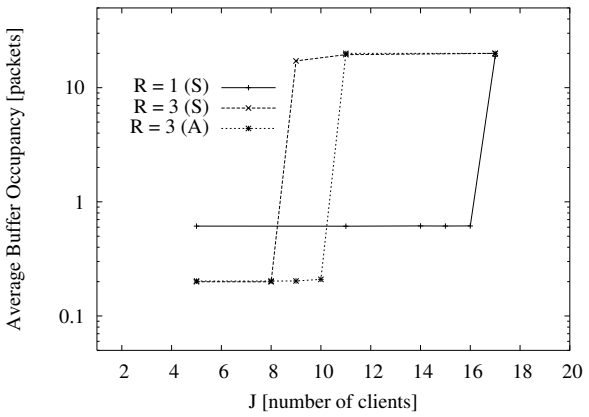

Fig. 15. Average buffer occupancy as a function of number of supported clients (flows) J for conventional ARQ ($R = 1$) and SMPT with $R = 3$ (bursty traffic with $\mu/(\lambda + \mu) = 0.4$, $1/\lambda = 10$, $B_{\max} = 20$ packets, Spreading Gain $G = 16$, and channel conditions $\alpha = 1/27$ and $\beta = 1/3$, fixed).

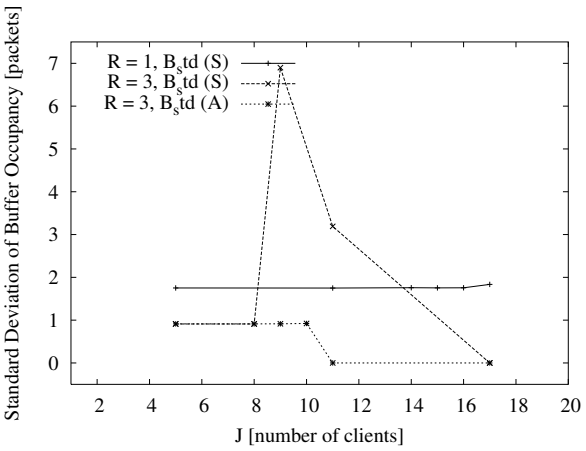

Fig. 16. Standard Deviation of buffer occupancy as a function of number of supported clients (flows) J for conventional ARQ ($R = 1$) and SMPT with $R = 3$ (bursty traffic with $\mu/(\lambda + \mu) = 0.4$ and $1/\lambda = 10$, $B_{\max} = 20$ packets, Spreading Gain $G = 16$, and channel conditions $\alpha = 1/27$ and $\beta = 1/3$, fixed).

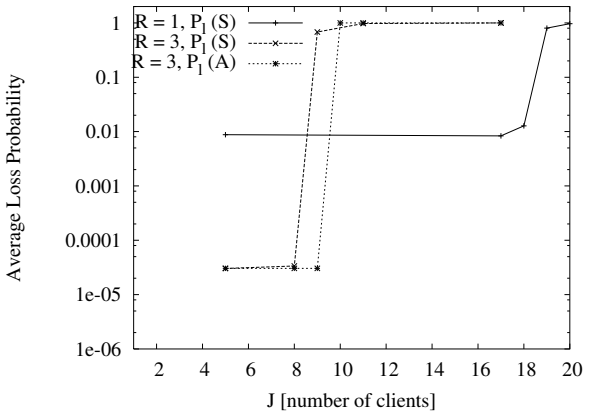

Fig. 17. Average loss probability as a function of number of supported clients (flows) J for conventional ARQ ($R = 1$) and SMPT with $R = 3$ (bursty traffic with $\mu/(\lambda + \mu) = 0.4$, $1/\lambda = 100$, $B_{\max} = 20$ packets, Spreading Gain $G = 16$, and channel conditions $\alpha = 1/27$ and $\beta = 1/3$, fixed).

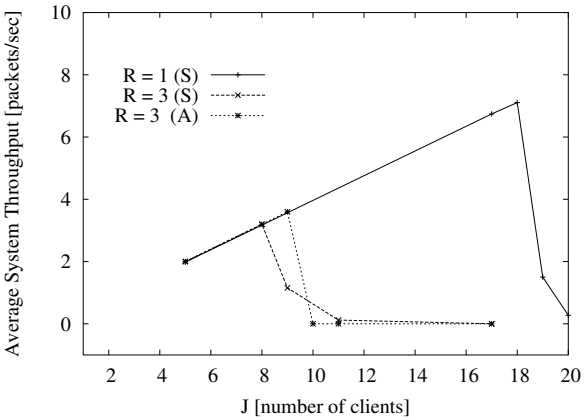

Fig. 18. Aggregate throughput as a function of number of supported clients (flows) J for conventional ARQ ($R = 1$) and SMPT with $R = 3$ (bursty traffic with $\mu/(\lambda+\mu) = 0.4$ and $1/\lambda = 100$, $B_{\max} = 20$ packets, Spreading Gain $G = 16$, and channel conditions $\alpha = 1/27$ and $\beta = 1/3$, fixed).

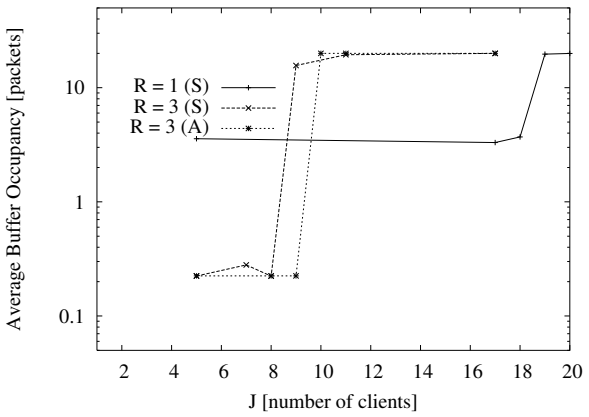

Fig. 19. Average buffer occupancy as a function of number of supported clients (flows) J for conventional ARQ ($R = 1$) and SMPT with $R = 3$ (bursty traffic with $\mu/(\lambda+\mu) = 0.4$, $1/\lambda = 100$, $B_{\max} = 20$ packets, Spreading Gain $G = 16$, and channel conditions $\alpha = 1/27$ and $\beta = 1/3$, fixed).

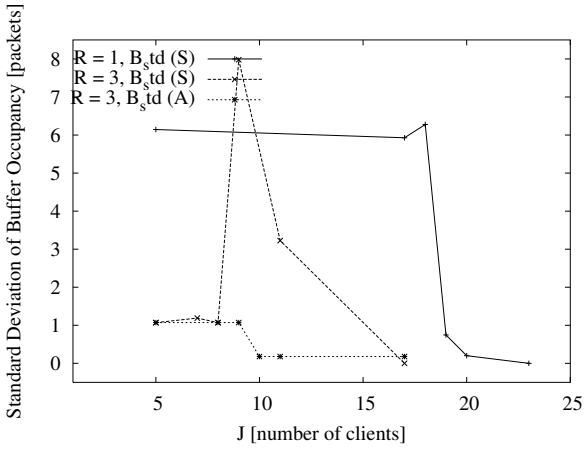

Fig. 20. Standard Deviation of buffer occupancy as a function of number of supported clients (flows) J for conventional ARQ ($R = 1$) and SMPT with $R = 3$ (bursty traffic with $\mu/(\lambda+\mu) = 0.4$ and $1/\lambda = 100$, $B_{\max} = 20$ packets, Spreading Gain $G = 16$, and channel conditions $\alpha = 1/27$ and $\beta = 1/3$, fixed).

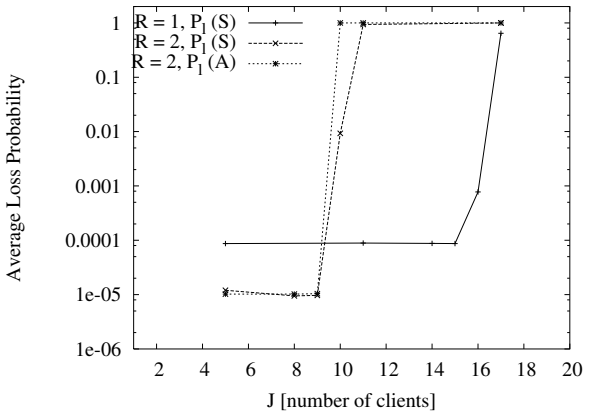

Fig. 21. Average loss probability as a function of number of supported clients (flows) J for conventional ARQ ($R = 1$) and SMPT with $R = 2$ (bursty traffic with $\mu/(\lambda+\mu) = 0.5$, $1/\lambda = 10$, $B_{\max} = 20$ packets, Spreading Gain $G = 16$, and channel conditions $\alpha = 1/27$ and $\beta = 1/3$, fixed).

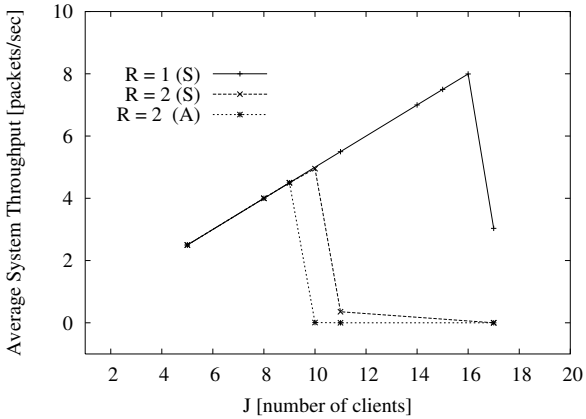

Fig. 22. Aggregate throughput as a function of number of supported clients (flows) J for conventional ARQ ($R = 1$) and SMPT with $R = 2$ (bursty traffic with $\mu/(\lambda+\mu) = 0.5$ and $1/\lambda = 10$, $B_{\max} = 20$ packets, Spreading Gain $G = 16$, and channel conditions $\alpha = 1/27$ and $\beta = 1/3$, fixed).

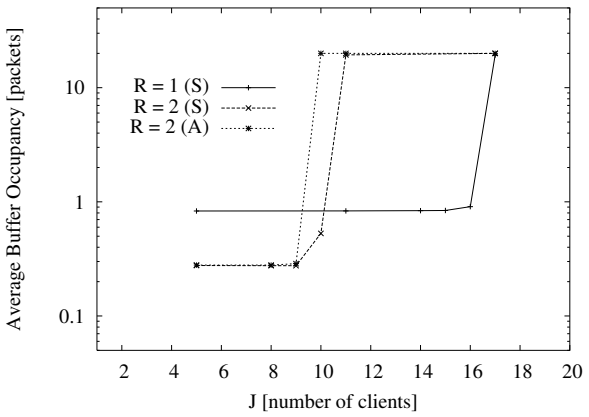

Fig. 23. Average buffer occupancy as a function of number of supported clients (flows) J for conventional ARQ ($R = 1$) and SMPT with $R = 2$ (bursty traffic with $\mu/(\lambda + \mu) = 0.5$, $1/\lambda = 10$, $B_{\max} = 20$ packets, Spreading Gain $G = 16$, and channel conditions $\alpha = 1/27$ and $\beta = 1/3$, fixed).

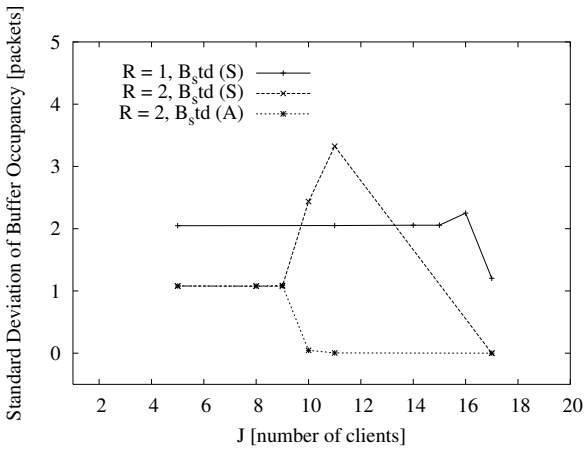

Fig. 24. Standard Deviation of buffer occupancy as a function of number of supported clients (flows) J for conventional ARQ ($R = 1$) and SMPT with $R = 2$ (bursty traffic with $\mu/(\lambda + \mu) = 0.5$ and $1/\lambda = 10$, $B_{\max} = 20$ packets, Spreading Gain $G = 16$, and channel conditions $\alpha = 1/27$ and $\beta = 1/3$, fixed).

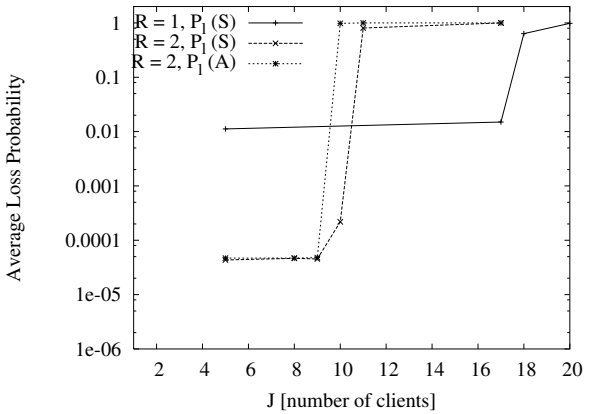

Fig. 25. Average loss probability as a function of number of supported clients (flows) J for conventional ARQ ($R = 1$) and SMPT with $R = 2$ (bursty traffic with $\mu/(\lambda + \mu) = 0.5$, $1/\lambda = 100$, $B_{\max} = 20$ packets, Spreading Gain $G = 16$, and channel conditions $\alpha = 1/27$ and $\beta = 1/3$, fixed).

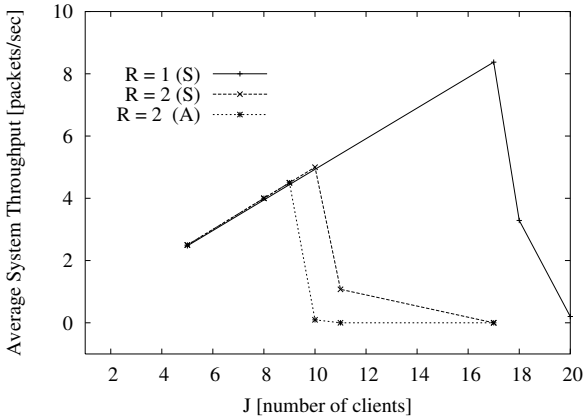

Fig. 26. Aggregate throughput as a function of number of supported clients (flows) J for conventional ARQ ($R = 1$) and SMPT with $R = 2$ (bursty traffic with $\mu/(\lambda+\mu) = 0.5$ and $1/\lambda = 100$, $B_{\max} = 20$ packets, Spreading Gain $G = 16$, and channel conditions $\alpha = 1/27$ and $\beta = 1/3$, fixed).

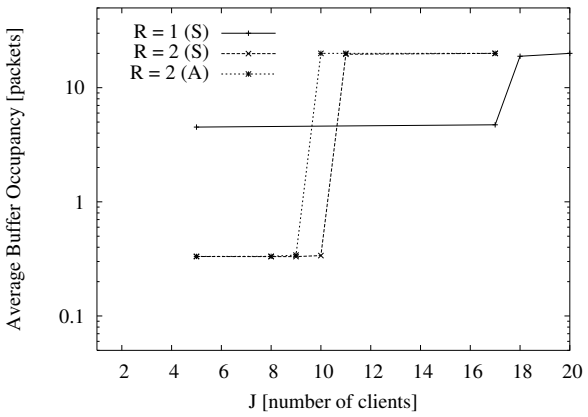

Fig. 27. Average buffer occupancy as a function of number of supported clients (flows) J for conventional ARQ ($R = 1$) and SMPT with $R = 2$ (bursty traffic with $\mu/(\lambda+\mu) = 0.5$, $1/\lambda = 100$, $B_{\max} = 20$ packets, Spreading Gain $G = 16$, and channel conditions $\alpha = 1/27$ and $\beta = 1/3$, fixed).

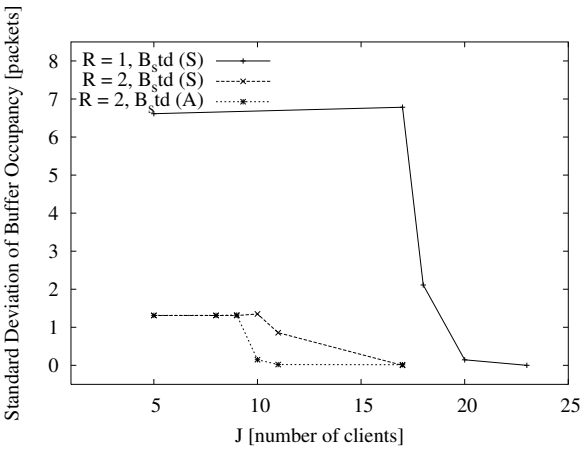

Fig. 28. Standard Deviation of buffer occupancy as a function of number of supported clients (flows) J for conventional ARQ ($R = 1$) and SMPT with $R = 2$ (bursty traffic with $\mu/(\lambda+\mu) = 0.5$ and $1/\lambda = 100$, $B_{\max} = 20$ packets, Spreading Gain $G = 16$, and channel conditions $\alpha = 1/27$ and $\beta = 1/3$, fixed).

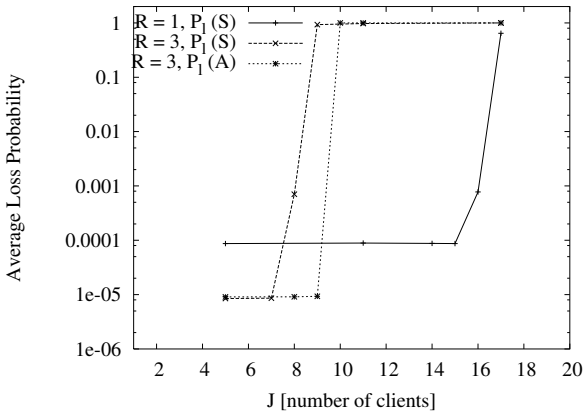

Fig. 29. Average loss probability as a function of number of supported clients (flows) J for conventional ARQ ($R = 1$) and SMPT with $R = 3$ (bursty traffic with $\mu/(\lambda+\mu) = 0.5$, $1/\lambda = 10$, $B_{\max} = 20$ packets, Spreading Gain $G = 16$, and channel conditions $\alpha = 1/27$ and $\beta = 1/3$, fixed).

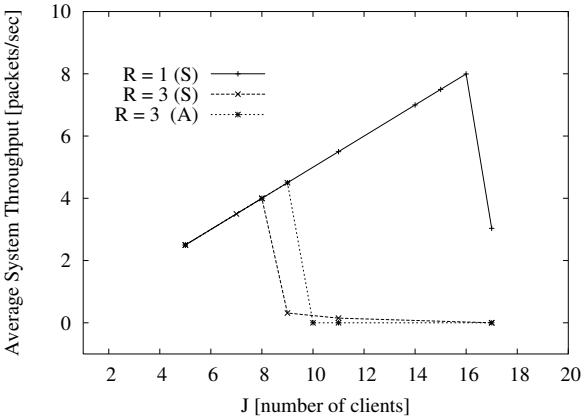

Fig. 30. Aggregate throughput as a function of number of supported clients (flows) J for conventional ARQ ($R = 1$) and SMPT with $R = 3$ (bursty traffic with $\mu/(\lambda+\mu) = 0.5$ and $1/\lambda = 10$, $B_{\max} = 20$ packets, Spreading Gain $G = 16$, and channel conditions $\alpha = 1/27$ and $\beta = 1/3$, fixed).

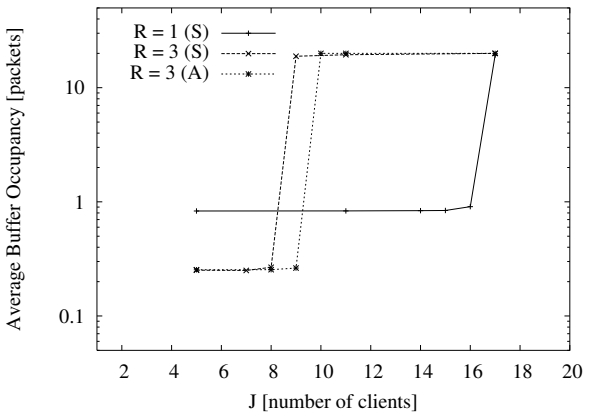

Fig. 31. Average buffer occupancy as a function of number of supported clients (flows) J for conventional ARQ ($R = 1$) and SMPT with $R = 3$ (bursty traffic with $\mu/(\lambda + \mu) = 0.5$, $1/\lambda = 10$, $B_{\max} = 20$ packets, Spreading Gain $G = 16$, and channel conditions $\alpha = 1/27$ and $\beta = 1/3$, fixed).

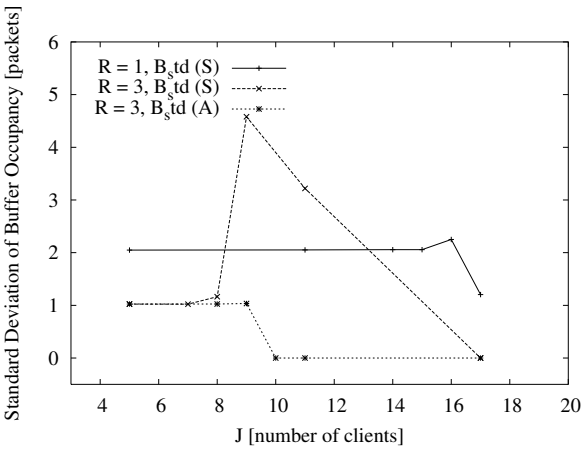

Fig. 32. Standard Deviation of buffer occupancy as a function of number of supported clients (flows) J for conventional ARQ ($R = 1$) and SMPT with $R = 3$ (bursty traffic with $\mu/(\lambda + \mu) = 0.5$ and $1/\lambda = 10$, $B_{\max} = 20$ packets, Spreading Gain $G = 16$, and channel conditions $\alpha = 1/27$ and $\beta = 1/3$, fixed).

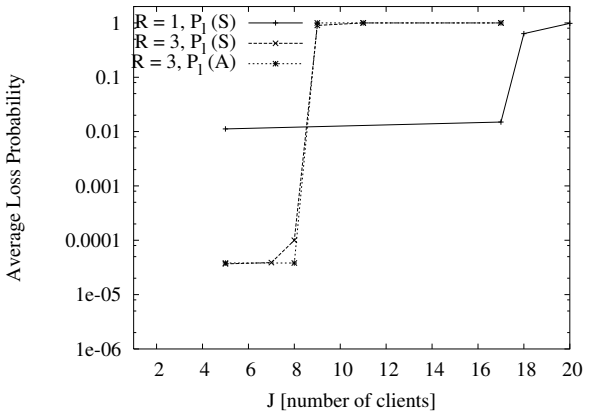

Fig. 33. Average loss probability as a function of number of supported clients (flows) J for conventional ARQ ($R = 1$) and SMPT with $R = 3$ (bursty traffic with $\mu/(\lambda + \mu) = 0.5$, $1/\lambda = 100$, $B_{\max} = 20$ packets, Spreading Gain $G = 16$, and channel conditions $\alpha = 1/27$ and $\beta = 1/3$, fixed).

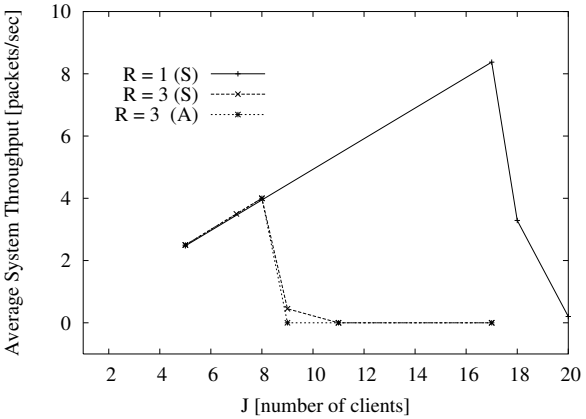

Fig. 34. Aggregate throughput as a function of number of supported clients (flows) J for conventional ARQ ($R = 1$) and SMPT with $R = 3$ (bursty traffic with $\mu/(\lambda+\mu) = 0.5$ and $1/\lambda = 100$, $B_{\max} = 20$ packets, Spreading Gain $G = 16$, and channel conditions $\alpha = 1/27$ and $\beta = 1/3$, fixed).

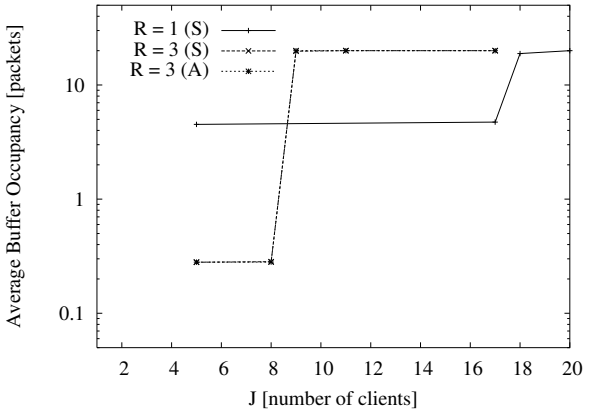

Fig. 35. Average buffer occupancy as a function of number of supported clients (flows) J for conventional ARQ ($R = 1$) and SMPT with $R = 3$ (bursty traffic with $\mu/(\lambda+\mu) = 0.5$, $1/\lambda = 100$, $B_{\max} = 20$ packets, Spreading Gain $G = 16$, and channel conditions $\alpha = 1/27$ and $\beta = 1/3$, fixed).

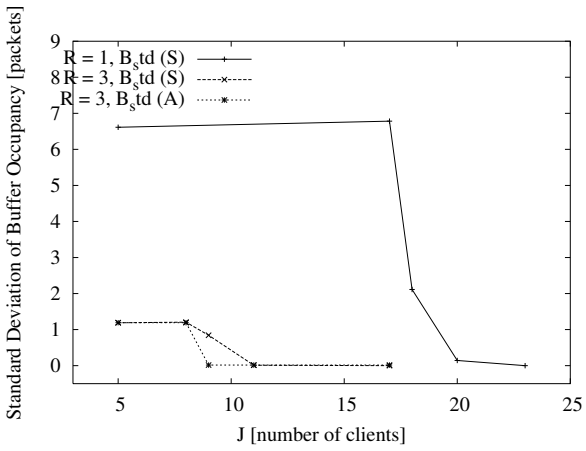

Fig. 36. Standard Deviation of buffer occupancy as a function of number of supported clients (flows) J for conventional ARQ ($R = 1$) and SMPT with $R = 3$ (bursty traffic with $\mu/(\lambda+\mu) = 0.5$ and $1/\lambda = 100$, $B_{\max} = 20$ packets, Spreading Gain $G = 16$, and channel conditions $\alpha = 1/27$ and $\beta = 1/3$, fixed).

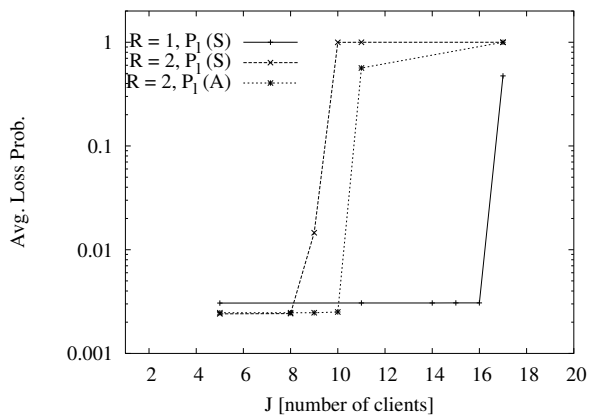

Fig. 37. Average loss probability as a function of number of supported clients (flows) J for conventional ARQ ($R = 1$) and SMPT with $R = 2$ (bursty traffic with $\mu/(\lambda + \mu) = 0.4$, $1/\lambda = 10$, $B_{\max} = 20$ packets, Spreading Gain $G = 16$, and channel conditions $\alpha = 1/100$ and $\beta = 1/10$, fixed).

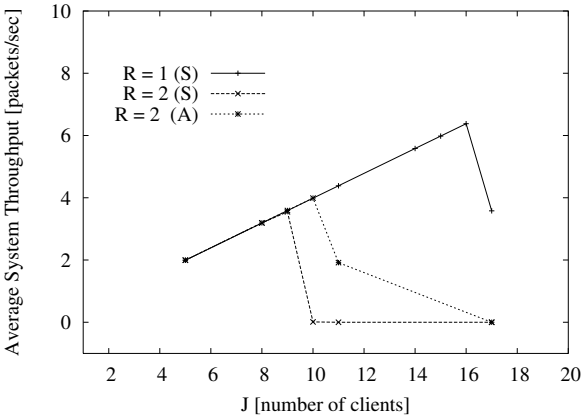

Fig. 38. Aggregate throughput as a function of number of supported clients (flows) J for conventional ARQ ($R = 1$) and SMPT with $R = 2$ (bursty traffic with $\mu/(\lambda+\mu) = 0.4$ and $1/\lambda = 10$, $B_{\max} = 20$ packets, Spreading Gain $G = 16$, and channel conditions $\alpha = 1/100$ and $\beta = 1/10$, fixed).

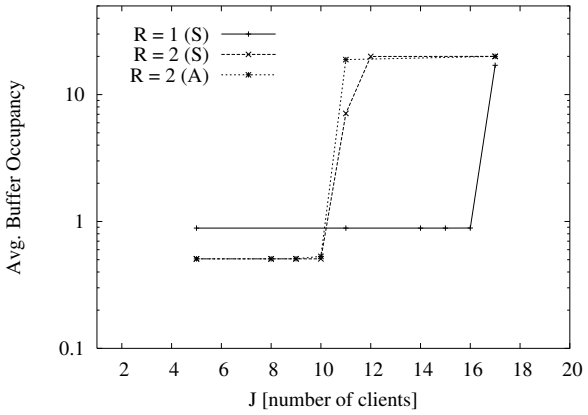

Fig. 39. Average buffer occupancy as a function of number of supported clients (flows) J for conventional ARQ ($R = 1$) and SMPT with $R = 2$ (bursty traffic with $\mu/(\lambda + \mu) = 0.4$, $1/\lambda = 10$, $B_{\max} = 20$ packets, Spreading Gain $G = 16$, and channel conditions $\alpha = 1/100$ and $\beta = 1/10$, fixed).

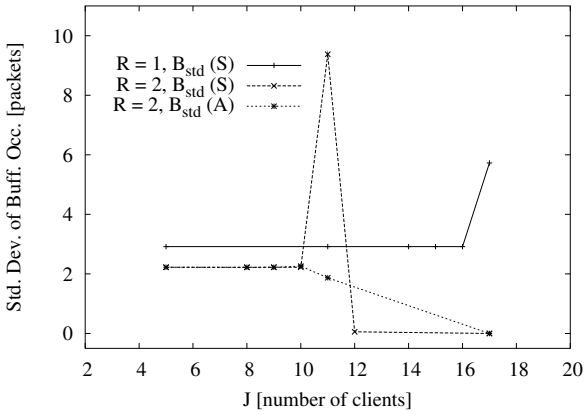

Fig. 40. Standard Deviation of buffer occupancy as a function of number of supported clients (flows) J for conventional ARQ ($R = 1$) and SMPT with $R = 2$ (bursty traffic with $\mu/(\lambda + \mu) = 0.4$ and $1/\lambda = 10$, $B_{\max} = 20$ packets, Spreading Gain $G = 16$, and channel conditions $\alpha = 1/100$ and $\beta = 1/10$, fixed).

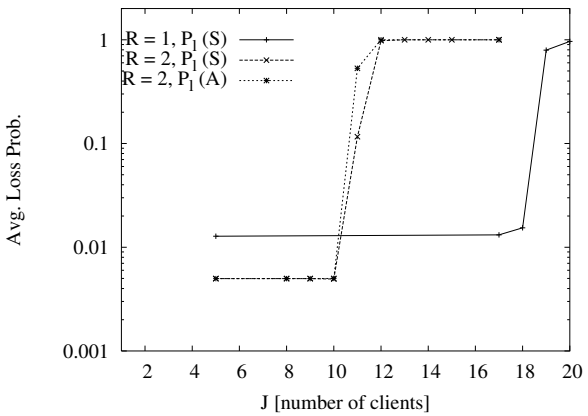

Fig. 41. Average loss probability as a function of number of supported clients (flows) J for conventional ARQ ($R = 1$) and SMPT with $R = 2$ (bursty traffic with $\mu/(\lambda + \mu) = 0.4$, $1/\lambda = 100$, $B_{\max} = 20$ packets, Spreading Gain $G = 16$, and channel conditions $\alpha = 1/100$ and $\beta = 1/10$, fixed).

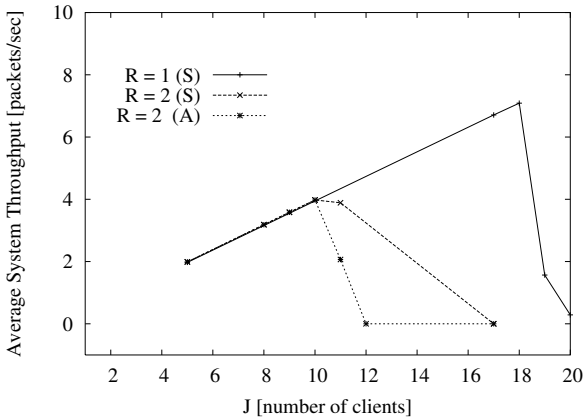

Fig. 42. Aggregate throughput as a function of number of supported clients (flows) J for conventional ARQ ($R = 1$) and SMPT with $R = 2$ (bursty traffic with $\mu/(\lambda+\mu) = 0.4$ and $1/\lambda = 100$, $B_{\max} = 20$ packets, Spreading Gain $G = 16$, and channel conditions $\alpha = 1/100$ and $\beta = 1/10$, fixed).

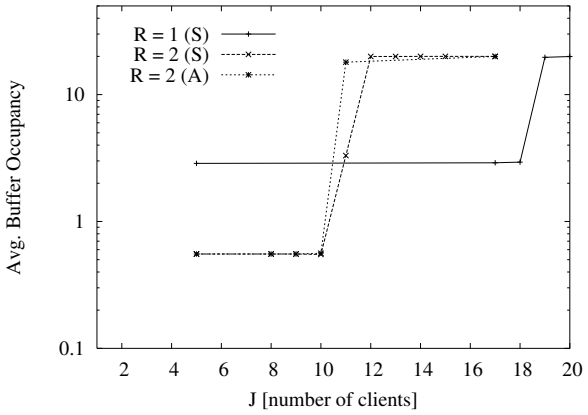

Fig. 43. Average buffer occupancy as a function of number of supported clients (flows) J for conventional ARQ ($R = 1$) and SMPT with $R = 2$ (bursty traffic with $\mu/(\lambda+\mu) = 0.4$, $1/\lambda = 100$, $B_{\max} = 20$ packets, Spreading Gain $G = 16$, and channel conditions $\alpha = 1/100$ and $\beta = 1/10$, fixed).

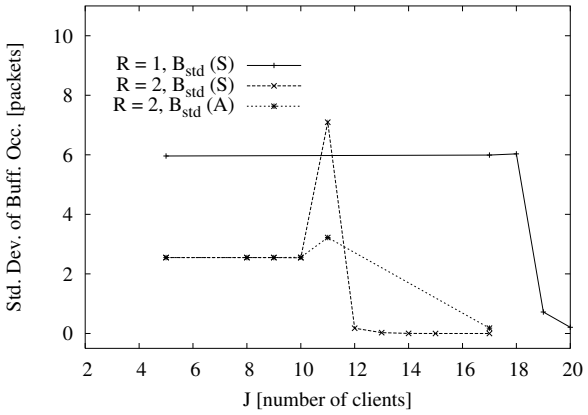

Fig. 44. Standard Deviation of buffer occupancy as a function of number of supported clients (flows) J for conventional ARQ ($R = 1$) and SMPT with $R = 2$ (bursty traffic with $\mu/(\lambda+\mu) = 0.4$ and $1/\lambda = 100$, $B_{\max} = 20$ packets, Spreading Gain $G = 16$, and channel conditions $\alpha = 1/100$ and $\beta = 1/10$, fixed).

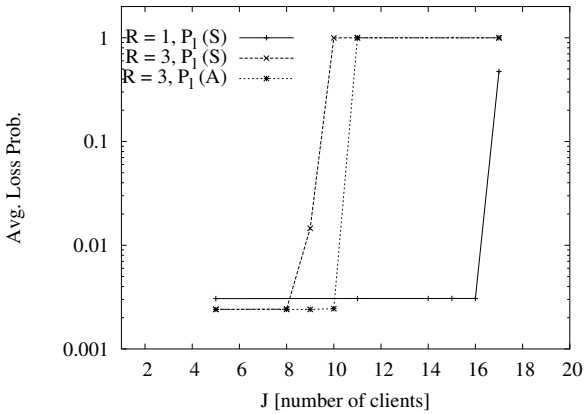

Fig. 45. Average loss probability as a function of number of supported clients (flows) J for conventional ARQ ($R = 1$) and SMPT with $R = 3$ (bursty traffic with $\mu/(\lambda+\mu) = 0.4$, $1/\lambda = 10$, $B_{\max} = 20$ packets, Spreading Gain $G = 16$, and channel conditions $\alpha = 1/100$ and $\beta = 1/10$, fixed).

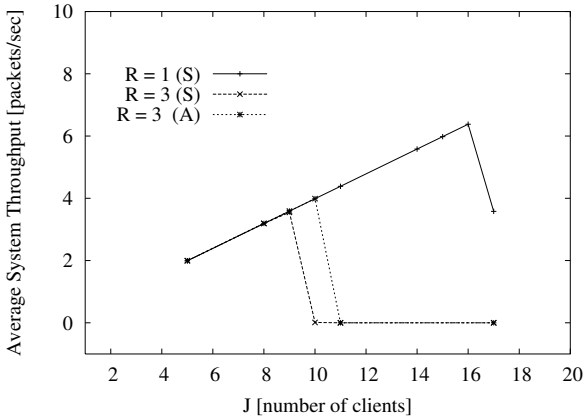

Fig. 46. Aggregate throughput as a function of number of supported clients (flows) J for conventional ARQ ($R = 1$) and SMPT with $R = 3$ (bursty traffic with $\mu/(\lambda+\mu) = 0.4$ and $1/\lambda = 10$, $B_{\max} = 20$ packets, Spreading Gain $G = 16$, and channel conditions $\alpha = 1/100$ and $\beta = 1/10$, fixed).

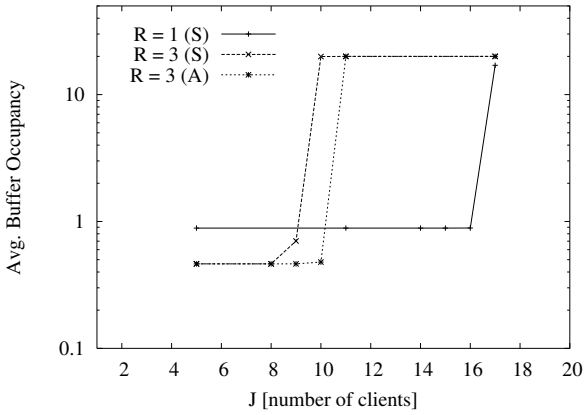

Fig. 47. Average buffer occupancy as a function of number of supported clients (flows) J for conventional ARQ ($R = 1$) and SMPT with $R = 3$ (bursty traffic with $\mu/(\lambda + \mu) = 0.4$, $1/\lambda = 10$, $B_{\max} = 20$ packets, Spreading Gain $G = 16$, and channel conditions $\alpha = 1/100$ and $\beta = 1/10$, fixed).

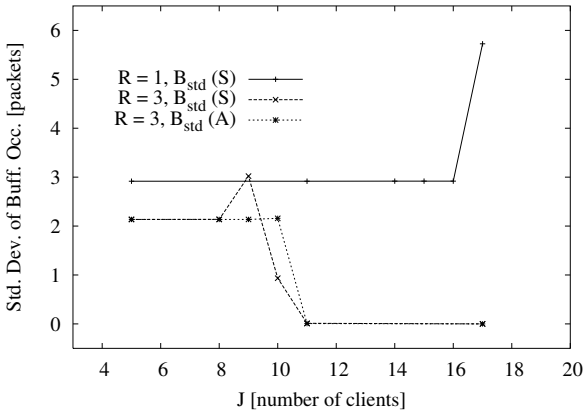

Fig. 48. Standard Deviation of buffer occupancy as a function of number of supported clients (flows) J for conventional ARQ ($R = 1$) and SMPT with $R = 3$ (bursty traffic with $\mu/(\lambda + \mu) = 0.4$ and $1/\lambda = 10$, $B_{\max} = 20$ packets, Spreading Gain $G = 16$, and channel conditions $\alpha = 1/100$ and $\beta = 1/10$, fixed).

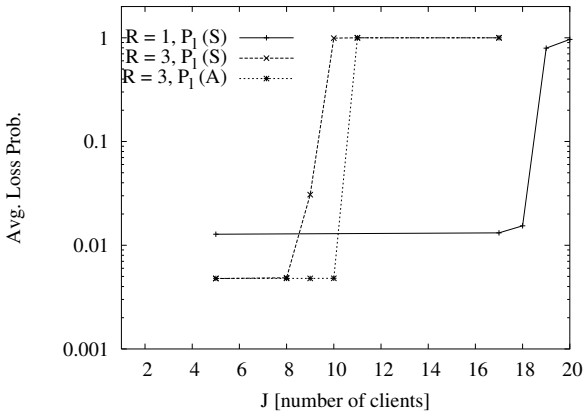

Fig. 49. Average loss probability as a function of number of supported clients (flows) J for conventional ARQ ($R = 1$) and SMPT with $R = 3$ (bursty traffic with $\mu/(\lambda + \mu) = 0.4$, $1/\lambda = 100$, $B_{\max} = 20$ packets, Spreading Gain $G = 16$, and channel conditions $\alpha = 1/100$ and $\beta = 1/10$, fixed).

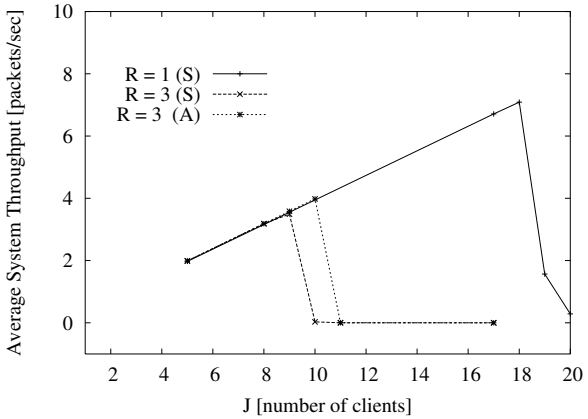

Fig. 50. Aggregate throughput as a function of number of supported clients (flows) J for conventional ARQ ($R = 1$) and SMPT with $R = 3$ (bursty traffic with $\mu/(\lambda+\mu) = 0.4$ and $1/\lambda = 100$, $B_{\max} = 20$ packets, Spreading Gain $G = 16$, and channel conditions $\alpha = 1/100$ and $\beta = 1/10$, fixed).

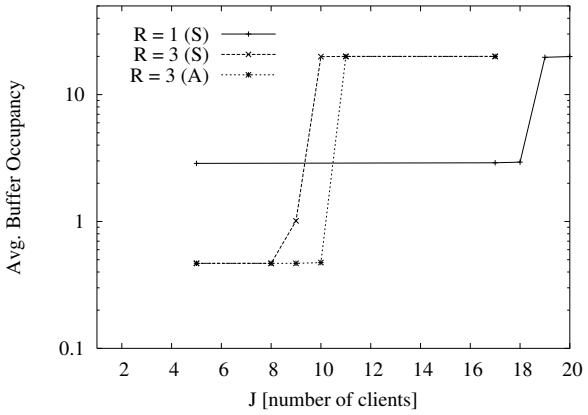

Fig. 51. Average buffer occupancy as a function of number of supported clients (flows) J for conventional ARQ ($R = 1$) and SMPT with $R = 3$ (bursty traffic with $\mu/(\lambda+\mu) = 0.4$, $1/\lambda = 100$, $B_{\max} = 20$ packets, Spreading Gain $G = 16$, and channel conditions $\alpha = 1/100$ and $\beta = 1/10$, fixed).

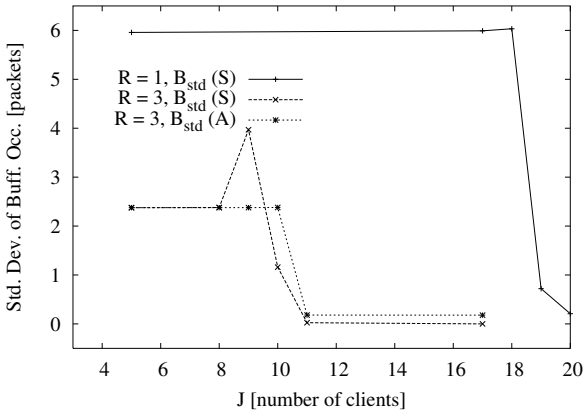

Fig. 52. Standard Deviation of buffer occupancy as a function of number of supported clients (flows) J for conventional ARQ ($R = 1$) and SMPT with $R = 3$ (bursty traffic with $\mu/(\lambda+\mu) = 0.4$ and $1/\lambda = 100$, $B_{\max} = 20$ packets, Spreading Gain $G = 16$, and channel conditions $\alpha = 1/100$ and $\beta = 1/10$, fixed).

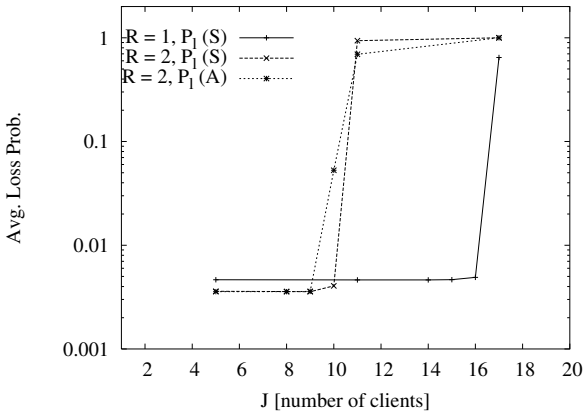

Fig. 53. Average loss probability as a function of number of supported clients (flows) J for conventional ARQ ($R = 1$) and SMPT with $R = 2$ (bursty traffic with $\mu/(\lambda+\mu) = 0.5$, $1/\lambda = 10$, $B_{\max} = 20$ packets, Spreading Gain $G = 16$, and channel conditions $\alpha = 1/100$ and $\beta = 1/10$, fixed).

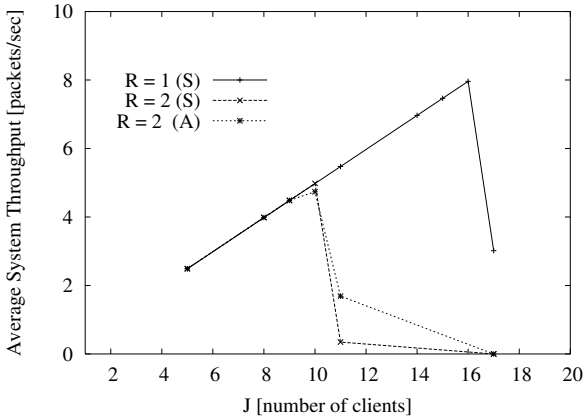

Fig. 54. Aggregate throughput as a function of number of supported clients (flows) J for conventional ARQ ($R = 1$) and SMPT with $R = 2$ (bursty traffic with $\mu/(\lambda+\mu) = 0.5$ and $1/\lambda = 10$, $B_{\max} = 20$ packets, Spreading Gain $G = 16$, and channel conditions $\alpha = 1/100$ and $\beta = 1/10$, fixed).

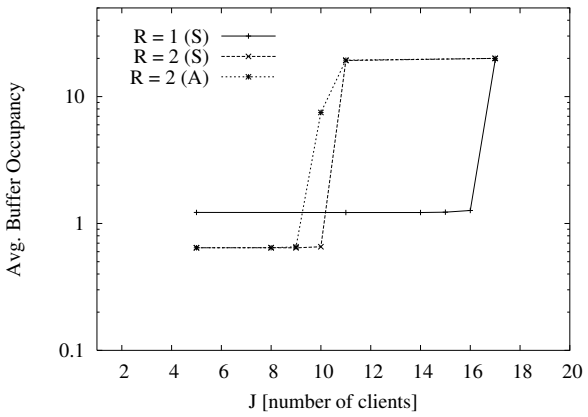

Fig. 55. Average buffer occupancy as a function of number of supported clients (flows) J for conventional ARQ ($R = 1$) and SMPT with $R = 2$ (bursty traffic with $\mu/(\lambda + \mu) = 0.5$, $1/\lambda = 10$, $B_{\max} = 20$ packets, Spreading Gain $G = 16$, and channel conditions $\alpha = 1/100$ and $\beta = 1/10$, fixed).

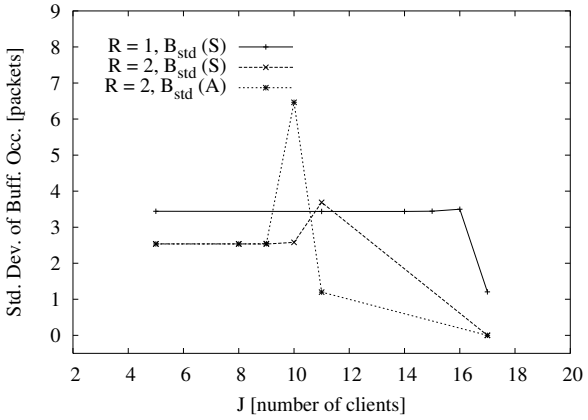

Fig. 56. Standard Deviation of buffer occupancy as a function of number of supported clients (flows) J for conventional ARQ ($R = 1$) and SMPT with $R = 2$ (bursty traffic with $\mu/(\lambda + \mu) = 0.5$ and $1/\lambda = 10$, $B_{\max} = 20$ packets, Spreading Gain $G = 16$, and channel conditions $\alpha = 1/100$ and $\beta = 1/10$, fixed).

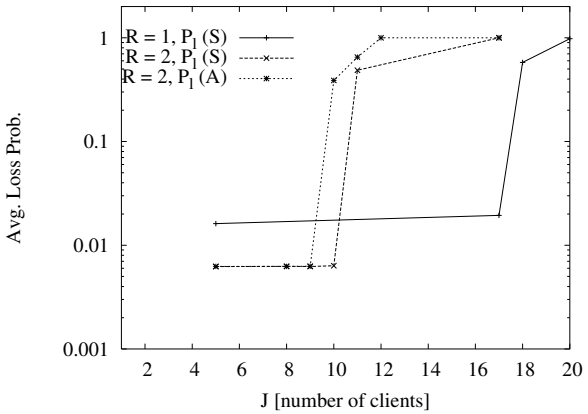

Fig. 57. Average loss probability as a function of number of supported clients (flows) J for conventional ARQ ($R = 1$) and SMPT with $R = 2$ (bursty traffic with $\mu/(\lambda + \mu) = 0.5$, $1/\lambda = 100$, $B_{\max} = 20$ packets, Spreading Gain $G = 16$, and channel conditions $\alpha = 1/100$ and $\beta = 1/10$, fixed).

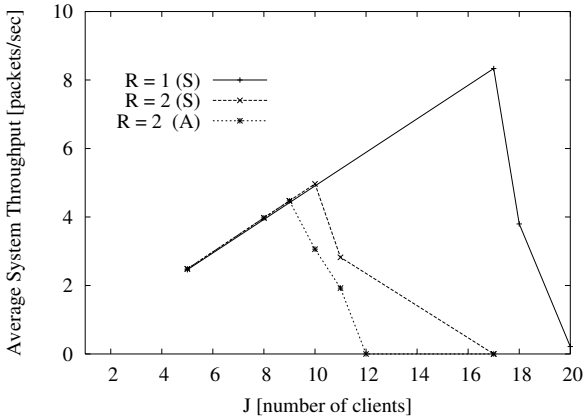

Fig. 58. Aggregate throughput as a function of number of supported clients (flows) J for conventional ARQ ($R = 1$) and SMPT with $R = 2$ (bursty traffic with $\mu/(\lambda+\mu) = 0.5$ and $1/\lambda = 100$, $B_{\max} = 20$ packets, Spreading Gain $G = 16$, and channel conditions $\alpha = 1/100$ and $\beta = 1/10$, fixed).

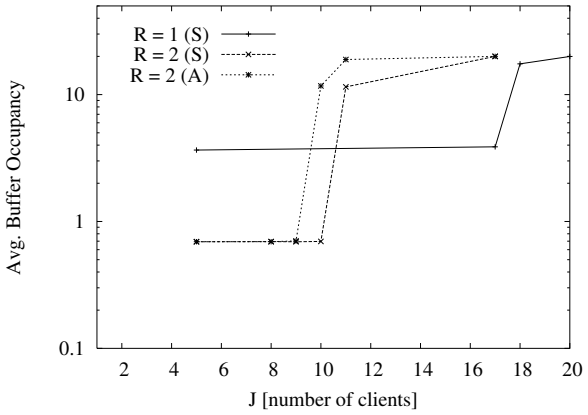

Fig. 59. Average buffer occupancy as a function of number of supported clients (flows) J for conventional ARQ ($R = 1$) and SMPT with $R = 2$ (bursty traffic with $\mu/(\lambda+\mu) = 0.5$, $1/\lambda = 100$, $B_{\max} = 20$ packets, Spreading Gain $G = 16$, and channel conditions $\alpha = 1/100$ and $\beta = 1/10$, fixed).

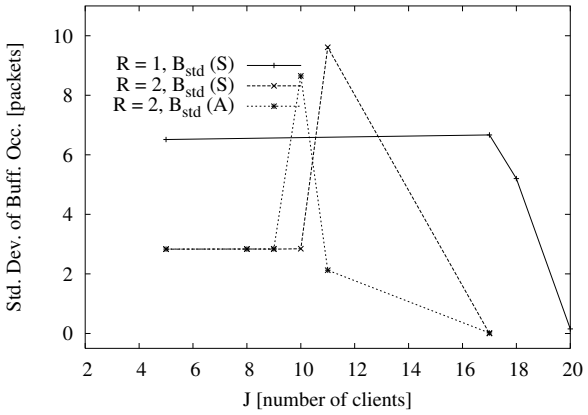

Fig. 60. Standard Deviation of buffer occupancy as a function of number of supported clients (flows) J for conventional ARQ ($R = 1$) and SMPT with $R = 2$ (bursty traffic with $\mu/(\lambda+\mu) = 0.5$ and $1/\lambda = 100$, $B_{\max} = 20$ packets, Spreading Gain $G = 16$, and channel conditions $\alpha = 1/100$ and $\beta = 1/10$, fixed).

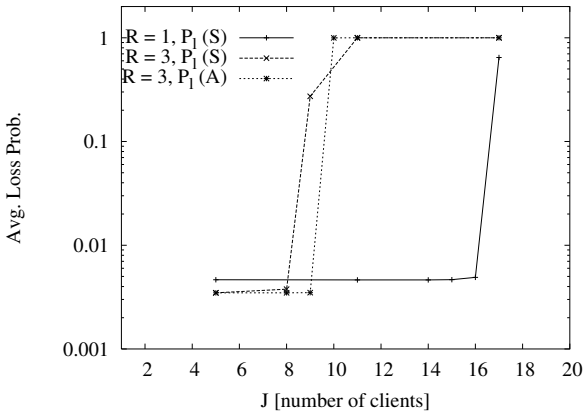

Fig. 61. Average loss probability as a function of number of supported clients (flows) J for conventional ARQ ($R = 1$) and SMPT with $R = 3$ (bursty traffic with $\mu/(\lambda+\mu) = 0.5$, $1/\lambda = 10$, $B_{\max} = 20$ packets, Spreading Gain $G = 16$, and channel conditions $\alpha = 1/100$ and $\beta = 1/10$, fixed).

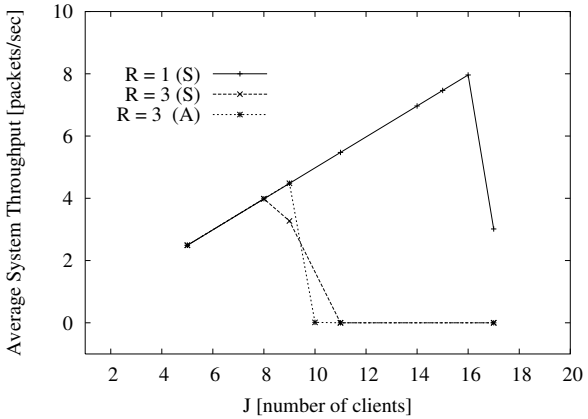

Fig. 62. Aggregate throughput as a function of number of supported clients (flows) J for conventional ARQ ($R = 1$) and SMPT with $R = 3$ (bursty traffic with $\mu/(\lambda+\mu) = 0.5$ and $1/\lambda = 10$, $B_{\max} = 20$ packets, Spreading Gain $G = 16$, and channel conditions $\alpha = 1/100$ and $\beta = 1/10$, fixed).

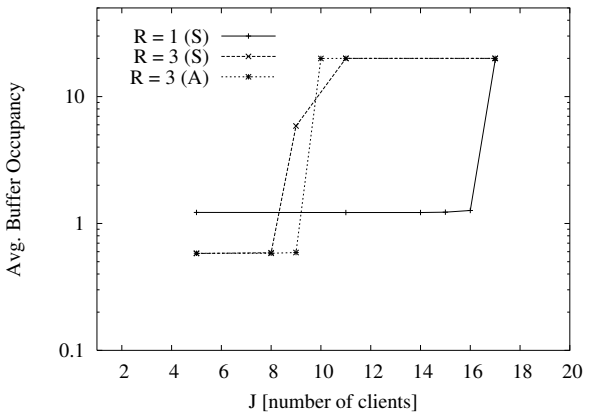

Fig. 63. Average buffer occupancy as a function of number of supported clients (flows) J for conventional ARQ ($R = 1$) and SMPT with $R = 3$ (bursty traffic with $\mu/(\lambda + \mu) = 0.5$, $1/\lambda = 10$, $B_{\max} = 20$ packets, Spreading Gain $G = 16$, and channel conditions $\alpha = 1/100$ and $\beta = 1/10$, fixed).

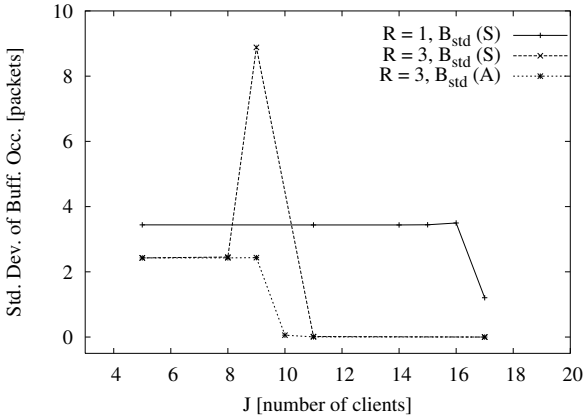

Fig. 64. Standard Deviation of buffer occupancy as a function of number of supported clients (flows) J for conventional ARQ ($R = 1$) and SMPT with $R = 3$ (bursty traffic with $\mu/(\lambda + \mu) = 0.5$ and $1/\lambda = 10$, $B_{\max} = 20$ packets, Spreading Gain $G = 16$, and channel conditions $\alpha = 1/100$ and $\beta = 1/10$, fixed).

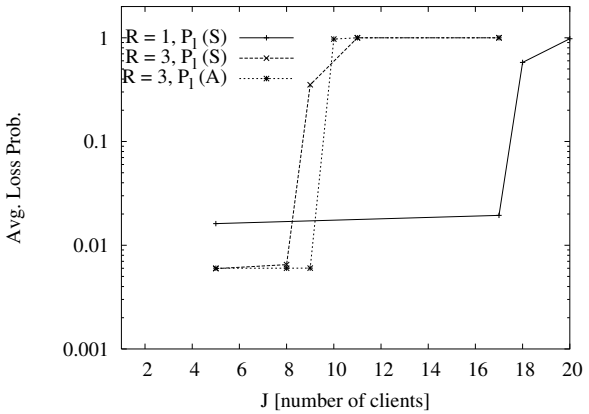

Fig. 65. Average loss probability as a function of number of supported clients (flows) J for conventional ARQ ($R = 1$) and SMPT with $R = 3$ (bursty traffic with $\mu/(\lambda + \mu) = 0.5$, $1/\lambda = 100$, $B_{\max} = 20$ packets, Spreading Gain $G = 16$, and channel conditions $\alpha = 1/100$ and $\beta = 1/10$, fixed).

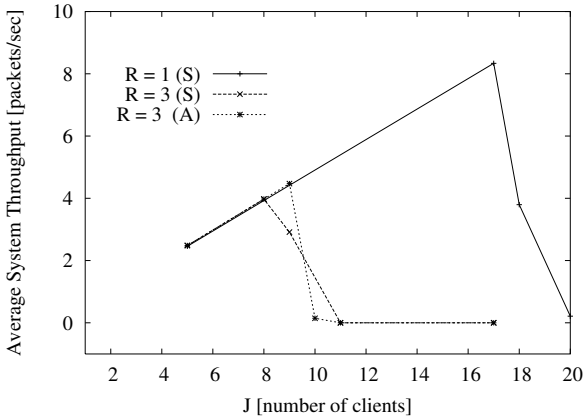

Fig. 66. Aggregate throughput as a function of number of supported clients (flows) J for conventional ARQ ($R = 1$) and SMPT with $R = 3$ (bursty traffic with $\mu/(\lambda+\mu) = 0.5$ and $1/\lambda = 100$, $B_{\max} = 20$ packets, Spreading Gain $G = 16$, and channel conditions $\alpha = 1/100$ and $\beta = 1/10$, fixed).

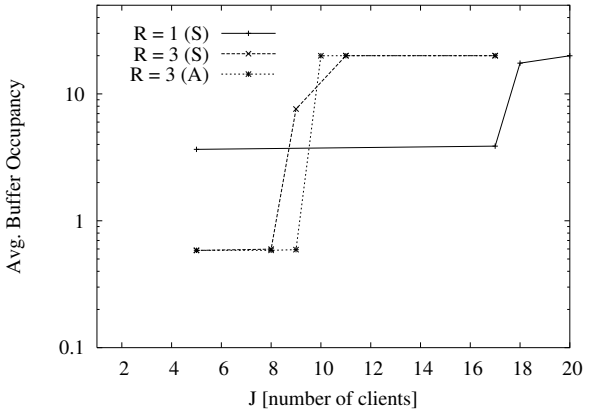

Fig. 67. Average buffer occupancy as a function of number of supported clients (flows) J for conventional ARQ ($R = 1$) and SMPT with $R = 3$ (bursty traffic with $\mu/(\lambda+\mu) = 0.5$, $1/\lambda = 100$, $B_{\max} = 20$ packets, Spreading Gain $G = 16$, and channel conditions $\alpha = 1/100$ and $\beta = 1/10$, fixed).

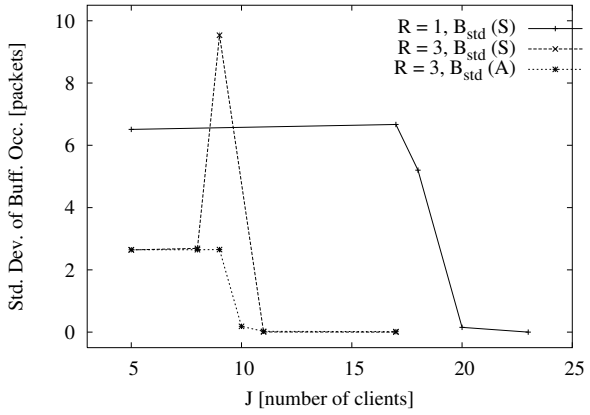

Fig. 68. Standard Deviation of buffer occupancy as a function of number of supported clients (flows) J for conventional ARQ ($R = 1$) and SMPT with $R = 3$ (bursty traffic with $\mu/(\lambda+\mu) = 0.5$ and $1/\lambda = 100$, $B_{\max} = 20$ packets, Spreading Gain $G = 16$, and channel conditions $\alpha = 1/100$ and $\beta = 1/10$, fixed).

Throughout we compare the performance of slow healing SMPT to the performance of conventional ARQ with $R = 1$.

We observe from the plots of average loss probability that in many scenarios that SMPT achieves significantly smaller loss probabilities and that both conventional ARQ and SMPT have very pronounced regions of stable and unstable operation. With both approaches the loss probability jumps abruptly from the values obtained for a small cell/cluster load (i.e., low interference) to a value close to one. We observe that within its stable region, SMPT provides significantly smaller loss probabilities than conventional ARQ provides in its stable region. This is due to the parallel transmissions in SMPT, which strive to keep the backlog low, as illustrated in Figs. 7, 11, 15, ..., 67. The smaller backlog in turn reduces the chance of losing a packet due to a full buffer. The smaller loss probabilities come at the expense of a smaller stability region. This is due to the usage of parallel CDMA codes with SMPT in response to packet drops on the wireless links. The parallel codes increase the interference level, which in turn tends to increase the probability of packet drops on the links, calling for the usage of even more parallel channels. These dynamics lead to instability when the load of the cell/cluster is beyond a critical threshold.

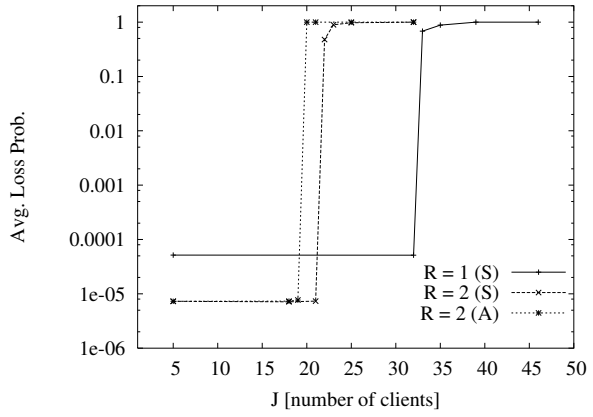

Fig. 69. Average loss probability as a function of number of supported clients(flows) J for conventional ARQ ($R = 1$) and SMPT with $R = 2$ for bursty traffic with average burst length $1/\lambda = 10$ packets, $\mu/(\lambda + \mu) = 0.4$, Spreading Gain $G = 32$, and channel conditions $\alpha = 1/27$ and $\beta = 1/3$, fixed.

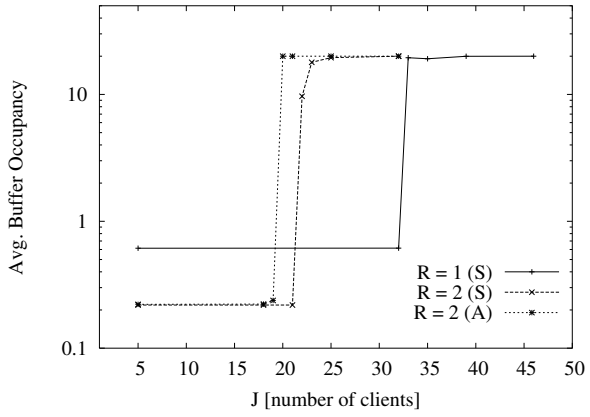

Fig. 70. Average loss probability as a function of number of supported clients(flows) J for conventional ARQ ($R = 1$) and SMPT with $R = 2$ for bursty traffic with average burst length $1/\lambda = 10$ packets, $\mu/(\lambda + \mu) = 0.4$, Spreading Gain $G = 32$, and channel conditions $\alpha = 1/27$ and $\beta = 1/3$, fixed.

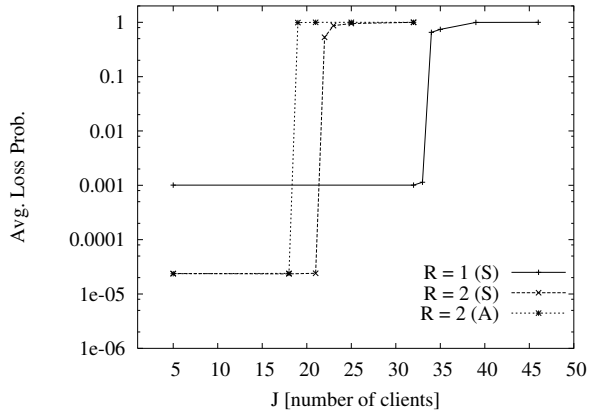

Fig. 71. Average loss probability as a function of number of supported clients(flows) J for conventional ARQ ($R = 1$) and SMPT with $R = 2$ for bursty traffic with average burst length $1/\lambda = 30$ packets, $\mu/(\lambda + \mu) = 0.4$, Spreading Gain $G = 32$, and channel conditions $\alpha = 1/27$ and $\beta = 1/3$, fixed.

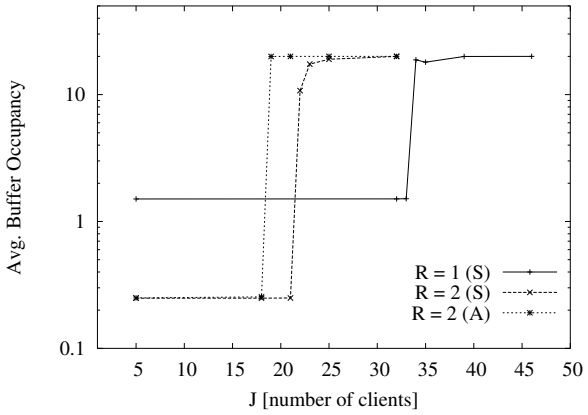

Fig. 72. Average loss probability as a function of number of supported clients(flows) J for conventional ARQ ($R = 1$) and SMPT with $R = 2$ for bursty traffic with average burst length $1/\lambda = 30$ packets, $\mu/(\lambda + \mu) = 0.4$, Spreading Gain $G = 32$, and channel conditions $\alpha = 1/27$ and $\beta = 1/3$, fixed.

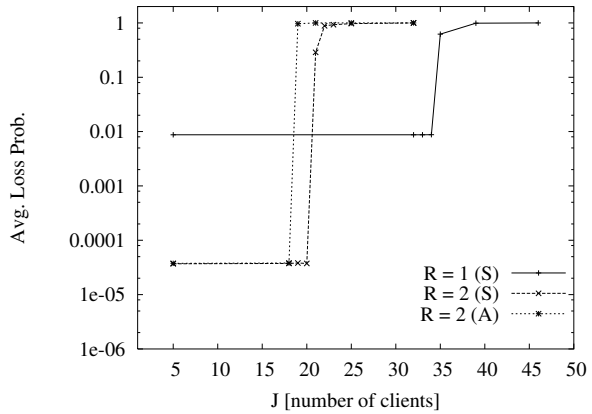

Fig. 73. Average loss probability as a function of number of supported clients(flows) J for conventional ARQ ($R = 1$) and SMPT with $R = 2$ for bursty traffic with average burst length $1/\lambda = 100$ packets, $\mu/(\lambda+\mu) = 0.4$, Spreading Gain $G = 32$, and channel conditions $\alpha = 1/27$ and $\beta = 1/3$, fixed.

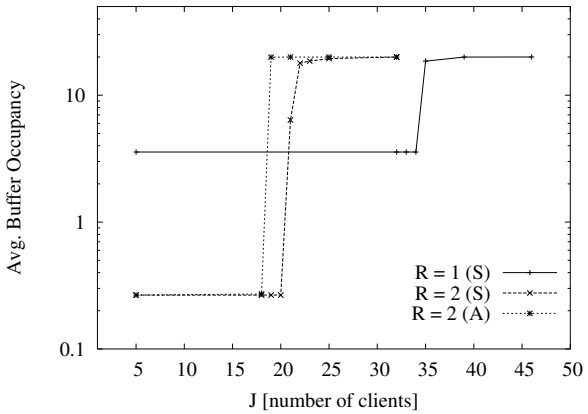

Fig. 74. Average loss probability as a function of number of supported clients(flows) J for conventional ARQ ($R = 1$) and SMPT with $R = 2$ for bursty traffic with average burst length $1/\lambda = 100$ packets, $\mu/(\lambda+\mu) = 0.4$, Spreading Gain $G = 32$, and channel conditions $\alpha = 1/27$ and $\beta = 1/3$, fixed.

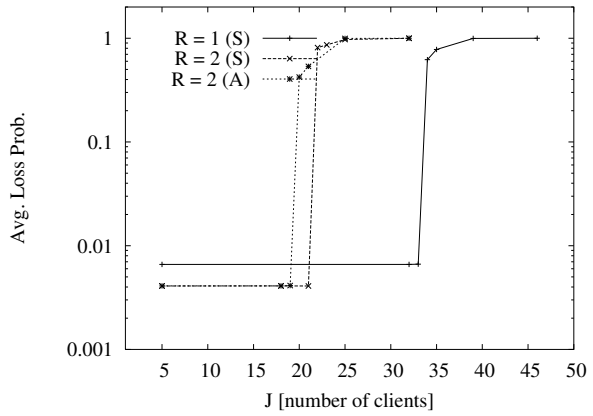

Fig. 75. Average loss probability as a function of number of supported clients(flows) J for conventional ARQ ($R = 1$) and SMPT with $R = 2$ for bursty traffic with average burst length $1/\lambda = 33.33$ packets, $\mu/(\lambda+\mu) = 0.4$, Spreading Gain $G = 32$, and channel conditions $\alpha = 1/100$ and $\beta = 1/10$, fixed.

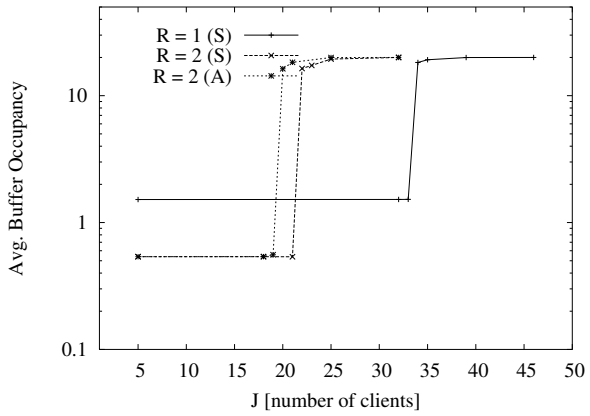

Fig. 76. Average loss probability as a function of number of supported clients(flows) J for conventional ARQ ($R = 1$) and SMPT with $R = 2$ for bursty traffic with average burst length $1/\lambda = 33.33$ packets, $\mu/(\lambda+\mu) = 0.4$, Spreading Gain $G = 32$, and channel conditions $\alpha = 1/100$ and $\beta = 1/10$, fixed.

Comparing Figs. 69, 71, 73, and 75, 77, and 79 we observe that the gap in the loss probability achieved by conventional ARQ and SMPT widens as the length of the traffic bursts increases. In the case of a system with channel parameters $\alpha = 1/27$ and $\beta = 1/3$, the gap widens from one order of magnitude for an average burst length of $1/\lambda = 10$ packets to over two and a half order of magnitudes for an average burst length of $1/\lambda = 100$ packets. This is due to the longer, more persistent packet bursts which typically can not fully be absorbed by the buffer and lead to a sharp increase of the loss probability with conventional ARQ. Note that the loss probability with conventional ARQ increases from around 10^{-4} to 10^{-2} as the average burst length increases from 10 to 100 packets. SMPT, on the other hand, by using multiple CDMA code channels makes up for packets that are dropped on the wireless links and stabilizes the throughput over the wireless link and experiences an increase in the loss probability of only about half an order of magnitude as the average burst length increases from 10 to 100 packets. We can also observe that the performance for R = 3 parallel codes is almost identical to the performance observed for up to R = 2 parallel codes. This indicates that low-cost mobile terminals with support for up to two parallel transmissions can extract essentially the full benefit from the class of SMPT ARQ mechanisms.

Although we do not explicitly study packet delay, the buffer occupancy results shown in Figs. 7, 11, etc., give an indication of the delays experienced with the conventional ARQ and SMPT link layers. We observe that in the stable region, SMPT achieves significantly smaller average buffer occupancies than conventional ARQ. We also observe that as the average burst length increases from 10 to 100 packets, the average buffer occupancy increases only from approximately 0.2 to approximately 0.3 with SMPT. With conventional ARQ, on the other hand, the average buffer occupancy increases from approximately 0.6 to 3.5 packets.

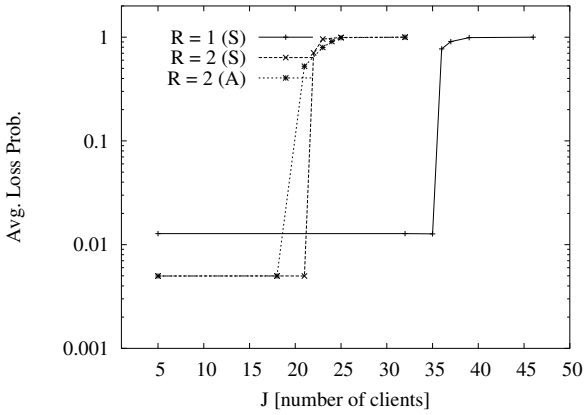

Fig. 77. Average loss probability as a function of number of supported clients(flows) J for conventional ARQ ($R = 1$) and SMPT with $R = 2$ for bursty traffic with average burst length $1/\lambda = 100$ packets, $\mu/(\lambda+\mu) = 0.4$, Spreading Gain $G = 32$, and channel conditions $\alpha = 1/100$ and $\beta = 1/10$, fixed.

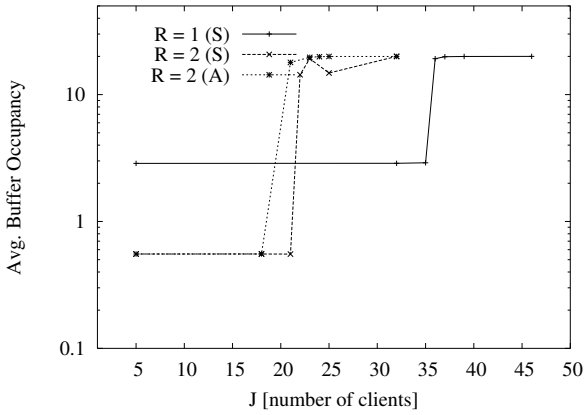

Fig. 78. Average loss probability as a function of number of supported clients(flows) J for conventional ARQ ($R = 1$) and SMPT with $R = 2$ for bursty traffic with average burst length $1/\lambda = 100$ packets, $\mu/(\lambda+\mu) = 0.4$, Spreading Gain $G = 32$, and channel conditions $\alpha = 1/100$ and $\beta = 1/10$, fixed.

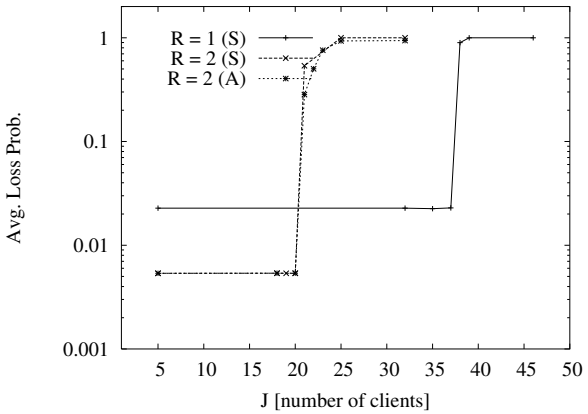

Fig. 79. Average loss probability as a function of number of supported clients(flows) J for conventional ARQ ($R = 1$) and SMPT with $R = 2$ for bursty traffic with average burst length $1/\lambda = 333.33$ packets, $\mu/(\lambda+\mu) = 0.4$, Spreading Gain $G = 32$, and channel conditions $\alpha = 1/100$ and $\beta = 1/10$, fixed.

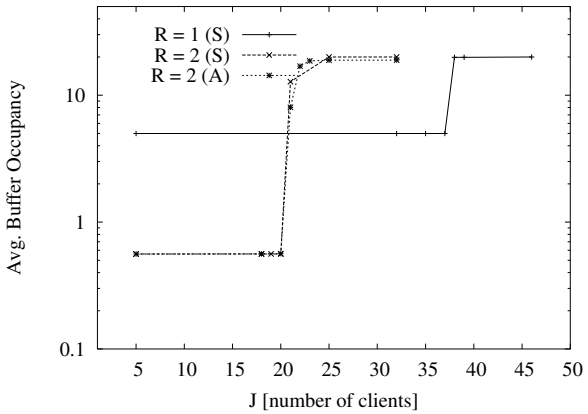

Fig. 80. Average loss probability as a function of number of supported clients(flows) J for conventional ARQ ($R = 1$) and SMPT with $R = 2$ for bursty traffic with average burst length $1/\lambda = 333.33$ packets, $\mu/(\lambda+\mu) = 0.4$, Spreading Gain $G = 32$, and channel conditions $\alpha = 1/100$ and $\beta = 1/10$, fixed.

This indicates the ability of SMPT to absorb a significant part of the increased burstiness and to maintain small buffer occupancies and correspondingly small delays for increased traffic burstiness. We can also observe the variability (standard deviation) of the buffer occupancy in Figs. 8, 12, 16, ..., 68. We found that in the stable region, SMPT achieves a significantly smaller standard deviation of the buffer occupancy (indicating smaller delay jitters) compared to conventional ARQ, whereby the difference in gain is most pronounced with more persistent traffic bursts.

We also observe from comparing the numerical results obtained from our analytical framework and the verifying simulation results that our analytical framework is highly accurate in predicting the loss probability and buffer occupancy in the stable region. Also, the analysis characterizes the range of the stable region with reasonably good accuracy, whereby the analysis conservatively underestimates the stable region by typically less than 10%.

V. Conclusion

We have developed a generalized analytical framework for assessing the link layer performance of Simultaneous MAC Packet Transmission (SMPT) mechanisms, a novel class of ARQ mechanisms. While the previously existing analytical framework for SMPT was limited to non-bursty Bernoulli packet traffic, our generalized analytical framework accommodates non-bursty as well as bursty packet traffic models. Our analytical framework is also general in the sense that new forms of SMPT, i.e., new policies for adjusting the number of used CDMA codes, can be analyzed by plugging a table with the new transition rules for the number of used code channels (replacing Table IV or V) into our analytical framework, which remains otherwise unchanged.

We have found that compared to conventional ARQ mechanisms which do not exploit the parallel code channels of multi-code CDMA, SMPT is effective in stabilizing the wireless link and in achieving small packet loss probabilities and small link buffer occupancies (and thus small delays) for bursty packet traffic in most of the scenarios. This improved link layer performance comes at the expense of a reduced number of packet flows that can be provided with the higher link layer QoS. This trade-off is modeled with good accuracy by our analytical framework, which can thus form a basis for admission control and resource allocation policies. Given a system scenario, we can determine the feasibility of employing SMPT using our analytical framework. In some scenarios, the capacity reduction outweighs the benefits obtained using SMPT (such as short burst lengths), during which the clients could resort to conventional ARQ instead of employing SMPT.

Several exciting avenues for future work on SMPT remain. One such avenue is to examine more complex packet service disciplines, e.g., service disciplines that exploit information from the higher protocol layers, e.g., playout deadlines of audio or video frames, to avoid the transport of packets that will miss their playout

deadline.

ACKNOWLEDGEMENT

We are grateful to Prof. Frank Fitzek of Aalborg University, Denmark, for insightful discussions at the early stages of this research.

REFERENCES

[1] M. Krishnam, M. Reisslein, and F. Fitzek, "Analytical framework for simultaneous MAC packet transmission (SMPT) in a multicode CDMA wireless system," *IEEE Transactions on Vehicular Technology*, vol. 53, no. 1, pp. 223–242, Jan. 2004.

[2] EIA/TIA-95 Rev. B, "Mobile station-base station compatibility standard for dual-mode wideband spread spectrum cellular systems," 1997.

[3] UMTS 30.03, "Universal Mobile Telecommunications System (UMTS); Selection Procedures for the Choice of Radio Transmission Technologies of the UMTS," .

[4] W. E. Leland, M. S. Taqqu, W. Willinger, and D. V. Wilson, "On the self-similar nature of ethernet traffic," *IEEE/ACM Transactions on Networking*, vol. 2, no. 1, pp. 1–15, Feb. 1994.

[5] J. Beran, R. Sherman, M. S. Taqqu, and W. Willinger, "Long-range dependence in variable-bit-rate video traffic," *IEEE Transactions on Communications*, vol. 43, no. 2, pp. 1566–1579, Feb. 1995.

[6] J. G. Kim and M. M. Krunz, "Bandwidth allocation in wireless networks with guaranteed packet loss performance," *IEEE Trans. Networking*, vol. 8, no. 3, pp. 337–349, June 2000.

[7] J. G. Kim and M. M. Krunz, "Delay analysis of Selective Repeat ARQ for a Markovian source over a wireless channel," *IEEE Trans. on Vehicular Tech.*, vol. 49, no. 5, pp. 1968–81, Sept. 2000.

[8] M. C. Chuah, B. Doshi, S. Dravida, R. Ejzak, and S. Nanda, "Link layer retransmission schemes for circuit-mode data over the CDMA physical channel," *Mobile Networks and Applications*, vol. 2, no. 2, pp. 195–211, Jan. 1997.

[9] M. M. Krunz and J. G. Kim, "Fluid analysis of delay and packet discard performance for QoS support in wireless networks," *IEEE Journal on Selected Areas in Communications*, vol. 19, no. 2, pp. 384–395, Feb. 2001.

[10] M. Zorzi, R. R. Rao, and L. B. Milstein, "ARQ error control for fading mobile radio channels," *IEEE Trans. on Vehicular Tech.*, vol. 46, no. 2, pp. 445–455, May 1997.

[11] P. Lettieri, C. Fragouli, and M.B. Srivastava, "Low power error control for wireless links," in *Proceedings of ACM/IEEE MobiCom '97*, 1997, pp. 139–150.

[12] H. Minn, M. Zeng, and V. K. Bhargava, "On ARQ scheme with adaptive error control," *IEEE Transactions on Vehicular Technology*, vol. 50, no. 6, pp. 1426–1436, Nov. 2001.

[13] S. Aramvith, C.-W. Lin, S. Roy, and M.-T. Sun, "Wireless video transport using conditional retransmission and low-delay interleaving," *IEEE Transactions on Circuits and Systems for Video Technology*, vol. 12, no. 6, pp. 558–565, June 2002.

[14] S. Choi and K. G. Shin, "A class of adaptive hybrid ARQ schemes for wireless links," *IEEE Transactions on Vehicular Technology*, vol. 50, no. 3, pp. 777–790, Mar. 2001.

[15] S.-H. Hwang, B. Kim, and Y.-S. Kim, "A hybrid ARQ scheme with power ramping," in *Proc. of IEEE Vehicular Technology Conference*, Fall 2001, pp. 1579–1583.

[16] P.-C. Hu, Z.-L. Zhang, and M. Kaveh, "Channel condition ARQ rate control for real-time wireless video under buffer constraints," in *Proceedings of IEEE International Conference on Image Processing*, 2000, pp. 124–127.

[17] H. Liu and M. El Zarki, "Performance of H.263 video transmission over wireless channels using hybrid ARQ," *IEEE Journal on Selected Areas in Communications*, vol. 15, no. 9, pp. 1775–1786, Dec. 1997.

[18] I. Joe, "An adaptive hybrid ARQ scheme with concatenated FEC codes for wireless ATM," in *Proceedings of ACM/IEEE MobiCom '97*, 1997, pp. 131–138.

[19] M. Shiwen, L. Shunan, S.S. Panwar, and Y. Wang, "Reliable transmission of video over ad-hoc networks using automatic repeat request and multipath transport," in *Proc. of IEEE Vehicular Technology Conference*, Fall 2001, pp. 615–619.

[20] K. Miyoshi, A. Matsumoto, C. Wengerter, M. Kasapidis, M. Uesugi, and O. Kato, "Constellation rearrangement and spreading code rearrangement for hybrid ARQ in MC-CDMA," in *Proceedings of IEEE International Symposium on Wireless Personal Multimedia Communications*, 2002, pp. 668–672.

[21] A. Majumdar, D. G. Sachs, I. V. Kozintsev, K. Ramchandran, and M.M. Yeung, "Multicast and unicast real-time video streaming over wireless LANs," *IEEE Transactions on Circuits and Systems for Video Technology*, vol. 12, no. 6, pp. 524–534, June 2002.

[22] J. Perez-Romero, R. Agusti, and O. Sallent, "Analysis of a type II hybrid ARQ strategy in a DS-CDMA packet transmission environment," *IEEE Transactions on Communications*, vol. 51, no. 8, pp. 1249–1253, Aug. 2003.

[23] T. Shoji, O. Kato, and M. Uesugi, "Wireless access method to ensure each user's QoS in unpredictable and various QoS requirements," *Wireless Personal Communications*, vol. 22, pp. 139–151, 2002.

[24] G. Wu, H. Harada, K. Taira, and Y. Hase, "An integrated transmission protocol for broadband mobile multimedia communication systems," in *Proc. of IEEE Vehicular Technology Conference*, 1997, pp. 1346–1350.

[25] M.-S. Do, Y. Park, and J.-Y. Lee, "Channel assignment with QoS guarantees for a multiclass multicode CDMA system," *IEEE Transactions on Vehicular Technology*, vol. 51, no. 5, pp. 934–948, Sept. 2002.

[26] M.R. Hueda, C. Rodriguez, and C. Marques, "Enhanced-performance video transmission in multicode CDMA wireless systems using a feedback error control scheme," in *Proceedings of IEEE Globecom*, San Antonio, TX, Nov. 2001, pp. 619–626.

[27] P.-R. Chang and C.-F. Lin, "Wireless ATM-based multicode CDMA transport architecture for MPEG-2 video transmission," *Proceedings of the IEEE*, vol. 87, no. 10, pp. 1807–1824, Oct. 1999.

[28] J. He, M. T. Liu, Y. Yang, and M. E. Muller, "A MAC protocol supporting wireless video transmission over multi-code CDMA personal communication networks," *Computer Communications*, vol. 21, no. 14, pp. 1256–1268, Sept. 1998.

[29] H. Liu, M.J. Karol, M. ElZarki, and K. Y. Eng, "Channel access and interference issues in multi-code DS-CDMA wireless packet (ATM) networks," *Wireless Networks*, vol. 2, no. 3, pp. 173–192, 1996.

[30] Z. Liu, M. Karol, M. ElZarki, and K. Eng, "Distributed-queuing request update multiple access (DQRUMA)," in *IEEE International Conference on Communications (ICC '96)*, Seattle, WA, June 1995, pp. 1224–1231.

[31] J. Chin-Lin and S. Nanda, "Load and interference based demand assignment (LIDA) for integrated services in CDMA wireless systems," Tech. Rep., Lucent Technologies, 1997.

[32] R.P. Ejzak, D.N. Knisely, S. Kumar, S. Laha, and S. Nanda, "BALI: A solution for high speed CDMA data," Tech. Rep., Bell Labs, 1997.

[33] C.-S. Chang and K.C. Chen, "Medium access protocol design for delay-guaranteed multicode CDMA multimedia networks," *IEEE Transactions on Wireless Communications*, vol. 2, no. 6, pp. 1159–1167, Nov. 2003.

[34] V. Huang and W. Zhuang;, "QoS-oriented packet scheduling for wireless multimedia CDMA communications," *IEEE Transactions on Mobile Computing*, vol. 3, no. 1, pp. 73–85, Jan. 2004.

[35] P.-Y. Kong, K.-C. Chua, and B. Bensaou, "A novel scheduling scheme to share dropping ratio while guaranteeing a delay bound in a MultiCode-CDMA network," *IEEE/ACM Transactions on Networking*, vol. 11, no. 6, pp. 994–1006, Dec. 2003.

[36] A. Stamoulis, N. D. Sidiropoulos, and G. B. Giannakis, "Time-varying fair queueing scheduling for multicode CDMA based on dynamic programming," *IEEE Transactions on Wireless Communications*, vol. 3, no. 2, pp. 512–523, Mar. 2004.

[37] L. Wang, Y.-K. Kwok, W.-C. Lau, and V.K.N. Lau, "Channel adaptive fair queueing for scheduling integrated voice and data services in multicode CDMA systems," in *Proceedings of IEEE Wireless Communications and Networking*, Mar. 2003.

[38] J. Sadowsky, "Voice and data traffic over the WCDMA air interface," Presentation at ASU, Apr. 2002, `http://www.eas.asu.edu/~trcsemnr/ASU_Talk.ppt`.

[39] F. Wegner, "Personal Communication. Siemens AG, Mobile Radio Access Simulation Group, Berlin, Germany," May 2000.

[40] E. N. Gilbert, "Capacity of a burst-noise channel," *Bell Systems Technical Journal*, vol. 39, pp. 1253–1266, Sept. 1960.

[41] E. O. Elliot, "Estimates of error rates for codes on burst-noise channels," *Bell Systems Technical Journal*, vol. 42, pp. 1977–1997, Sept. 1963.

[42] P. Bhagwat, P. Bhattacharya, A. Krishna, and S. K. Tripathi, "Using channel state dependent packet scheduling to improve TCP throughput over wireless LANs," *ACM Wireless Networks*, vol. 3, pp. 91–102, 1997.

[43] H. S. Wang and N. Moayeri, "Finite-state markov model – a useful model for radio communication channels," *IEEE Transactions on Vehicular Technology*, vol. 44, pp. 163–177, Feb. 1995.

[44] M. Zorzi and R.R. Rao, "Error-Constrained Error Control for Wireless Channels," *IEEE Personal Communications*, pp. 27–33, Dec. 1997.

[45] M. Zorzi, R. R. Rao, and L. B. Milstein, "On the accuracy of a first-order markovian model for data block transmission on fading channels," in *Proceedings of IEEE International Conference on Universal Personal Communications*, Nov. 1995, pp. 211–215.

[46] M. Zorzi, R. R. Rao, and L. B. Milstein, "Error statistics in data transmissions over fading channels," *IEEE Transactions on Communications*, vol. 46, no. 11, pp. 1468–77, Nov. 1998.

[47] R. R. Rao, "Higher Layer Perspectives on Modeling the Wireless Channel," in *Proc. of IEEE Information Theory Workshop*, 1998.

[48] J. Holtzman, "A Simple, Accurate Method to Calculate Spread Spectrum Multiple Access Error Probabilities," *IEEE Trans. Commun.*, vol. 40, no. 3, pp. 461–464, Mar. 1992.